ADVANCED CHARACTERIZATION OF PEROVSKITE SOLAR CELLS ENABLING TOP-CELL APPLICATION IN TANDEMS

MRINAL ABHINAV

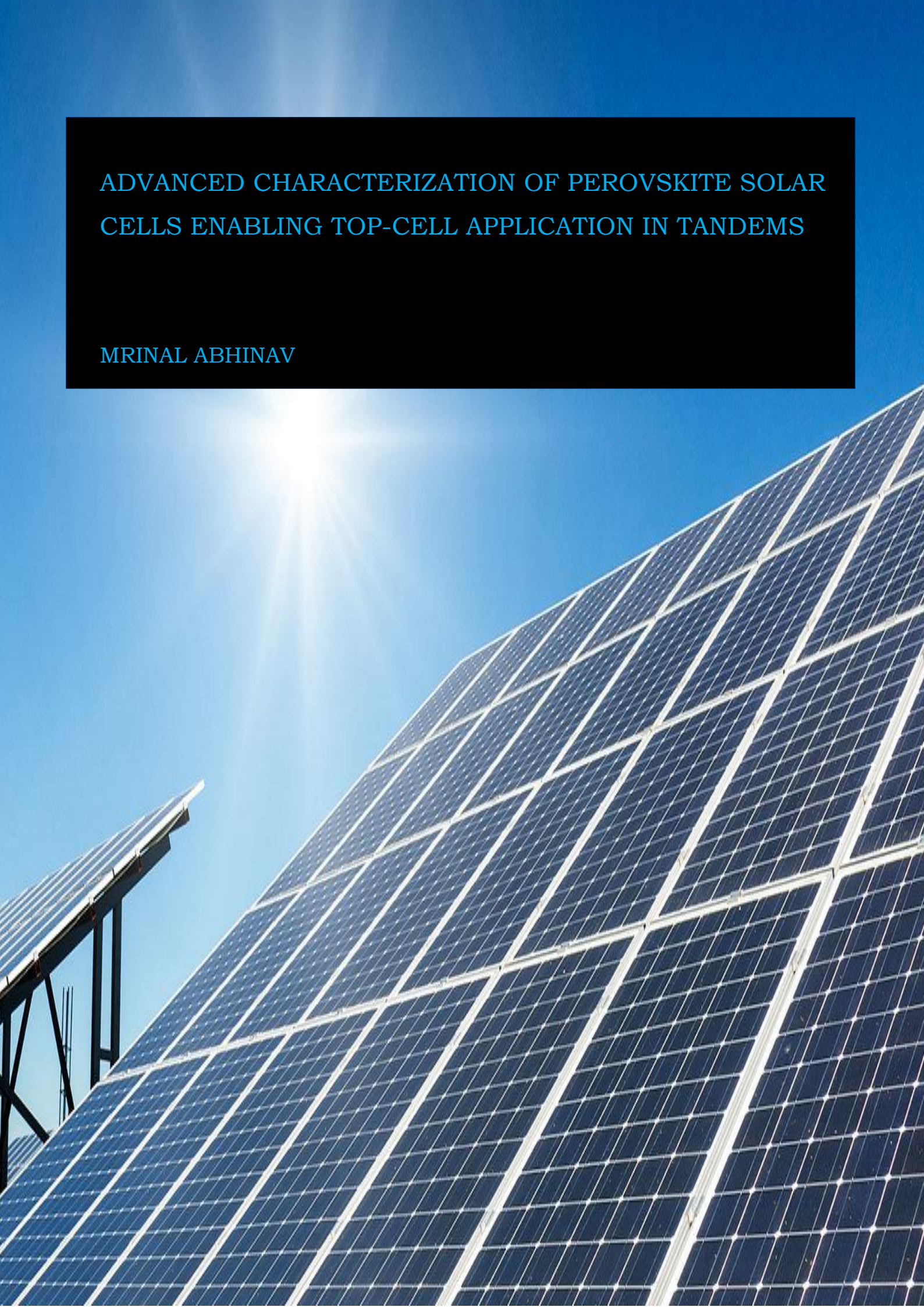

Advanced Characterization Of Perovskite Solar Cells Enabling Top-Cell Applications In Tandems

by

Mrinal Abhinav

to obtain the degree of

Master of Science

at the Delft University of Technology,

to be defended publicly on 23rd, August, 2021 at 10:00 AM.

Student number:	5065747	
Project duration:	November 13, 2020 – August 5, 2021	
Thesis committee:	Prof. Dr. Arthur Weeber,	TU Delft, Supervisor
	Prof. Dr. Arno Smets,	TU Delft, Professor
	Dr. Ir. Mohamad Ghaffarian Niasar,	TU Delft, Assistant Professor
	Drs. Petra Manshanden,	TNO, Daily Supervisor

This thesis is confidential and cannot be made public until December 31, 2023

An electronic version of this thesis is available at http://repository.tudelft.nl/.

TU Delft Delft University of Technology

PVMD Delft University of Technology

TNO innovation for life

Abstract

Perovskite solar cells (PSCs) have a high potential in PV systems, with total power conversion efficiencies (PCEs) of single junction PSC reaching up to 25.52%. Because of the fast growth of PCE, PSCs has become the emerging star of the PV industry which piqued the attention of the research community. The fact that they can be used as a top cell in a tandem perovskite-Si design further adds to their potential. However, for perovskites to be effective in the solar industry, scalability and stability must also be considered. For a long time, the stability of PSCs has been a major source of concern. Thus, it is important to observe the performance of perovskite carefully in laboratory to understand the behavior under real-world, and thus operational, conditions.

Therefore, this work is focused on characterizing several properties and behavior of perovskite devices important for these operational conditions: series resistance losses, behavior under different temperature and illumination levels and a protocol for maximum power point tracking (MMPT).

- Suns-Voc method is done primarily to understand the power loss mechanism, especially series resistance can be easily computed using this method. The analysis of Suns-Voc (Jsc-Voc) requires the validity of superposition principle to hold. The experiments were done to prove the validity of principle and the results indicate that the superposition principle does not hold for perovskite devices.
- The perovskite module was subjected to various temperature (15°C to 55°C) and illumination levels (100% to 11% of 1 Sun). From these measurements, absolute and normalized temperature coefficients were calculated and compared to published values in the literature.
- The true maximum power point (MPP) is the most critical aspect to consider in order to ensure that the PV module harvests maximum power at all operating points. Thus, to obtain the maximum power output under outdoor conditions where MPP fluctuates with temperature and irradiation, MPPT is used. A new measurement protocol has been proposed and implemented to track the true MPP of perovskite module. The result obtained from this method were as accurate as the standard J-V measurements.

The studies and tests conducted in this paper may be useful in providing a better understanding of PSCs in real-world operational circumstances.

Acknowledgement

This work is part of my MSc thesis in SET (Sustainable Energy Technology) at TU Delft. First and foremost, I would like to thank my supervisors, Prof. Dr. Gianluca Coletti and Prof. Dr. Arthur Weeber, for providing me with valuable suggestion and mentoring me. I am grateful to Drs. Petra Manshanden for being such a pleasant and inspiring daily supervisor at TNO, Petten. The project would not have been as effective without her. She helped me comprehend some new ideas and aided me when I encountered difficulties. I would like to thank team members of tandem group at TNO, Petten and at Solliance partners TNO, Eindhoven for their feedbacks during our meeting. I am also thankful to the members of PVMD group at TU Delft for their critical and valuable comments during my review meeting.

My thanks also go to Arno Smets and Mohamad Ghaffarian Niasar for agreeing to be my graduate committee. I owe my gratitude to my parents for their love and support, as well as for being such a source of inspiration in my life. Lastly I would like to thank my friends here in Netherlands and also in India for constantly motivating me. This project would not have been accomplished without the encouragement I received from my friends anytime I was feeling down.

Mrinal Abhinav
Delft, August 2021

Contents

List of Figures

List of Tables

1 Introduction

The document reports the thesis work done at TNO, location Petten, Netherlands with support from TNO, Eindhoven. This chapter aims to set the perspective and will relate the work to the current main problem. Climate change is unquestionably one of the most pressing issues confronting our generation. The chapter starts with the associated problems due to climate change and the importance of energy transition and briefly discusses the solution to the problem. Solar photovoltaic (PV) will play an important role in energy transition along with other renewable energy technologies. The research contributes to enhance the deployment of PV technologies by investigating some factors related to tandem PV devices. Subsequently, the perovskite solar cells and the problems associated are also briefly explained. Thereafter, the chapter ends with the outline of this report.

1.1. Background

Energy demand is expected to rise by 28 percent from 169 PWh in 2015 to 216 PWh in 2040, owing to the rising global population and economy[9]. Despite the fact that renewable energy is growing at the fastest rate in the world, the major amount of energy (around 80%) is expected to be produced by fossil fuel burning in 2040[9].

Although burning fossil fuels is a simple way to produce power, it has negative consequences on our planet. The combustion of fossil fuels, particularly unpurified coals, emits pollutants and dust into the atmosphere. Emissions of greenhouse gases have the ability to trigger climate change and global warming, which could severely harm the atmosphere and endanger human activity's protection. On the other hand, pollution from coal dust poses a serious threat to public health. According to the Intergovernmental Panel on Climate Change(IPCC), the fossil fuel emissions are the primary contributor to global warming[52]. Emissions from fossil fuel and industry accounted for 89% global emission of CO_2 in 2018[52]. In 2019, the global mean of atmospheric CO_2 concentration was 409 ppm as shown in Figure 1.1[49].

Renewable energy is a way to resolve the issue of energy scarcity while also reducing the environmental effect of the existing energy system. Hydropower, geothermal energy, wind energy, and solar energy are all examples of renewable energy. Solar energy is the most abundant of all renewable energy sources. Every year, the Sun provides the Earth's surface with 10^8 TWh of energy, of which we actually extract 442 TWh[34]. As a result, solar energy's potential, including PV (photovoltaic), appears to be nearly infinite, and the abundant solar energy can be converted into energy that can be utilized as electricity.

The photovoltaic effect is the direct conversion of sunlight into electrical power using a semiconductor based device called a solar cell. The proportion of sunlight that illuminates the solar cell and

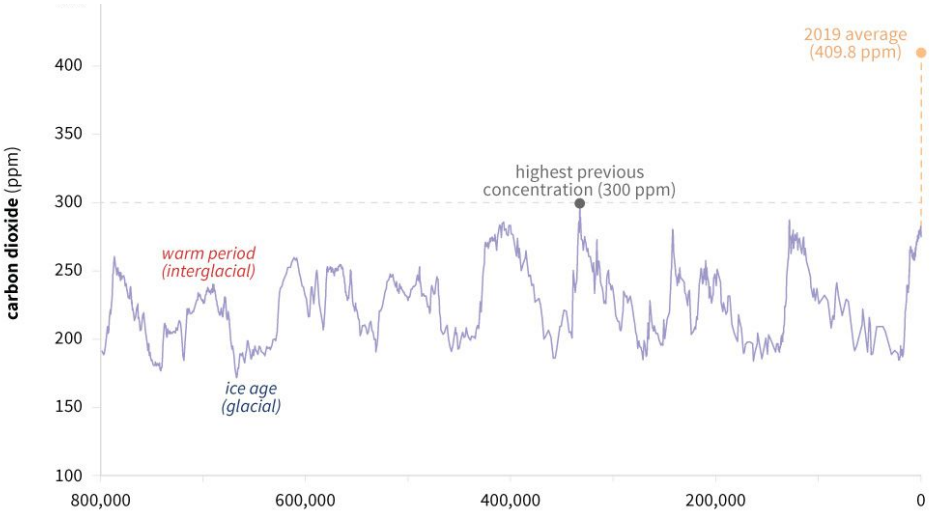

Figure 1.1: Global atmospheric carbon dioxide concentrations (CO2) in parts per million (ppm) for the past 800,000 years [49]

getting converted into electricity is given by a term known as Power conversion efficiency(PCE). There are several factors affecting the PCE such as operation location and ambient conditions, technology of fabrication, composition of absorber layer.

Besides sustainability, the economic feasibility of the energy technologies is determined by the cost of the power generation, which is given by LCOE (levelized cost of electricity).The LCOE is calculated by dividing the total lifecycle cost of a technology by the total lifetime energy production. Thus, there is a need to reduce the LCOE of PV technology which can be ensured by increasing the PCE of the solar cells. Figure 1.2 shows the comparison of generation cost of electricity using solar and other power sources. The PCE of solar cells must be also be improved in order to expand the use of renewable energy. The higher PCE will also result in decreasing the pay back period, thus making this parameter crucial for the increasing the share of PV power as a source of global electricity. The area required for the installation and the materials for mounting system will be less with technologies of high PCE. This results in reducing the airborne pollutants, emissions and will improve the environmental profile of the PV system.

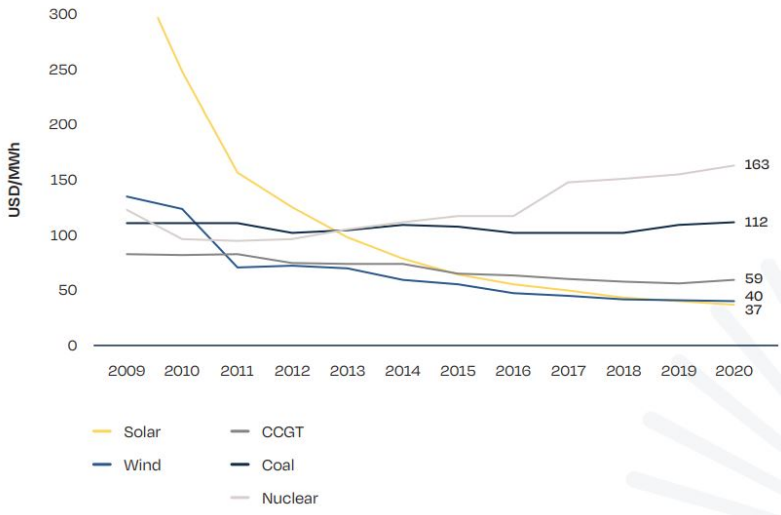

Figure 1.2: LCOE values of different power sources from 2009 to 2020 [23]

The PCE is limited by the theoretical Shockley-Quisser (SQ) limit for a p–n single junction solar cell. Under one sun irradiance, the closest PCE to SQ Limit by any solar cell is around 29% which is made of GaAs (III-V), [92],[30]. But, large-scale production of these solar cells is prohibitively expensive. Solar cells made of crystalline silicon (c-Si) which is the second most abundant element available, dominate the terrestrial PV sector. Under 1 Sun illumination, the maximum PCE achieved for single-junction c-Si is 26.7% which is very close to the practical limit of such solar cells[94],[30].

As it can be seen from Figure 1.3, thermalization losses are experienced by photons with energy above the absorber's bandgap (32.6% of overall solar radiation is accounted and is depicted in the grey region) and the energy of the photons which are below the bandgap are unable to be absorbed (as shown in the pink region of the figure)[96]. Multi-junction solar cells also known as tandem devices, which are made up of several light-absorbing layers with different bandgaps, have been shown to reduce these losses.

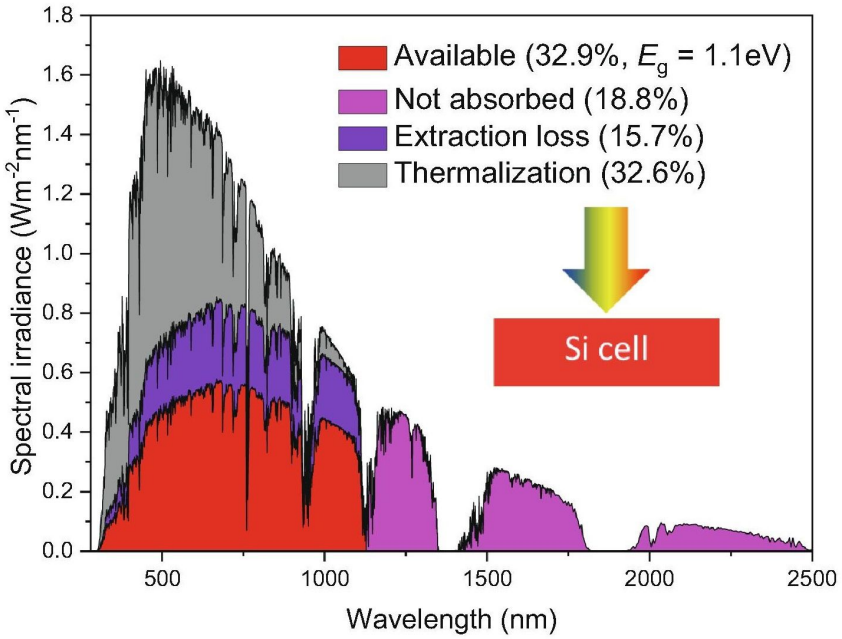

Figure 1.3: Solar spectrum of single junction Si solar cell [96]

1.2. Tandem PV

Tandem solar cells are made up of two or more than two subcell that are stacked on top of each other. Each subcell in the tandem can be adjusted to a particular part of the solar spectrum since the different subcells capture complementary parts of the solar spectrum. The top layer of PV cell with a wide bandgap absorbs photons having high energy while allowing photons with low energy to pass which are absorbed by the bottom layer of PV cell as they are of smaller bandgap material. By capturing photons of high energy in the top layer and photons of lower energy in the bottom layer, the tandem cell's cumulative PCE exceeds that of a single junction solar cell. Figure 1.4 represents the device structure of a typical tandem cell where top cell absorbs the higher energy photons (purple region of solar spectrum) and Si as a bottom cell, absorbs the remaining energy available after passing through the top cell(depicted as red region in the figure)[96].

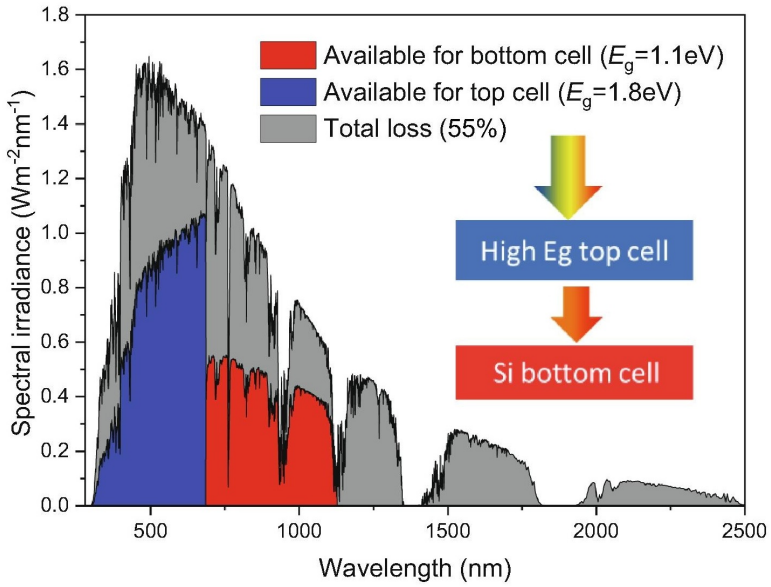

Figure 1.4: Solar spectrum of tandem solar cell with Si as a bottom cell [96]

Solar cells can achieve efficiencies upto 43% for two-junction and 50% for three-junction[7] as compared to an efficiency limit of 31% for single-junction solar cells, according to the fundamental Shockley-Queisser (SQ) limit[73]. Thus, using tandems on silicon solar cells is a promising way to improve their performance. Using tandem device of III-V/Si solar cell by stacking mechanically, an efficiency of 32.8% was obtained and an efficiency of 35.9% was achieved for three junction[22]. The high price of III-V solar cell growth technology makes large-scale terrestrial applications difficult. Given the dominance of c-Si solar cells in the terrestrial PV industry, introducing a low-cost absorber on top of the c-Si to produce high-efficiency tandem solar cells would be a more promising method to reduce the LCOE. The introduction of emerging solar cells and their rapid advancement has proven advantageous and they are now being used in tandem as a combination with existing PV technologies.

There has been a rapid development in the research of metal halide perovskites solar cells in the recent past. The PCE of single junction perovskite solar cell has risen from 3.8% to 25.5% [36] in a decade[1],[45]. Some features of the perovskite solar cell such as bandgap tuning, solution processing at low cost, long diffusion length and high carrier mobility makes perovskites an excellent option to use in tandems. Recently, a record breaking efficiency of 29.52% was achieved by Oxford PV on perovskite/Si tandem cell having an area of 1.12cm^2[60].

1.2.1. Tandem architecture

Different tandem cell configurations are possible depending on the subcell design and bonding technique, such as a tandem cell with 2T(two terminal), 3T(three terminal), or 4T(four terminal). Tandem device with 3T is not discussed in this report.

2T tandem is also known as monolithic tandem having two external electrodes whereas 4T tandem has 4 external electrodes. The architecture of 2T and 4T tandems are shown in Figure 1.5

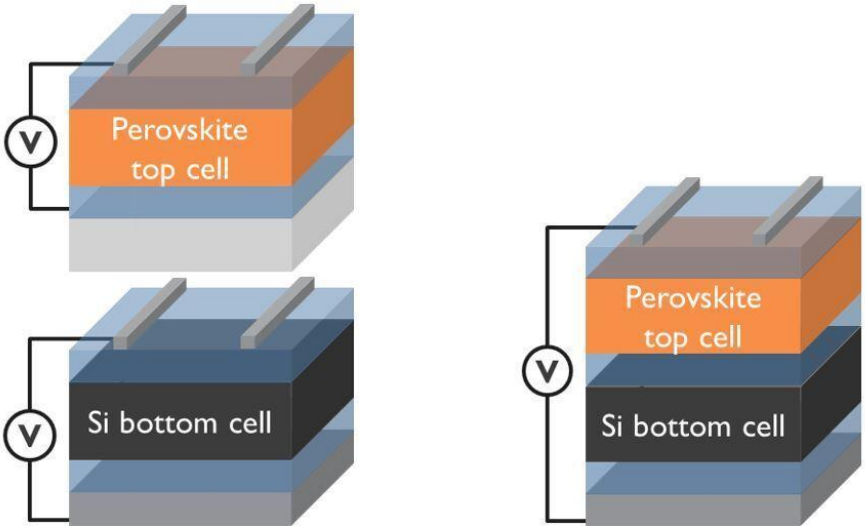

Figure 1.5: Schematic representation of the two main tandem architectures; Four-terminal (4T) configuration (left) and Two terminal (2T) configuration(right)[3]

Monolithical connection is made by the by the recombination or tunneling junction for each subcell in a 2T tandem. The 2T tandem devices are series connected and thus the photocurrents of subcell should be equal to each other. The parallel connection of the 2T tandem devices are also possible which requires voltage matching. If not, the efficiency of 2T tandem devices will decrease because of the subcell of lower photocurrent. Since the subcells in 4T tandems are electrically isolated, there is no current matching limitation[90]. In 4T, there are four electrodes compared to the two electrode in 2T tandem. Out of four electrode, three of which must be broadband transparent and strongly conductive.

1.2.2. Tandem combinations

Different combinations of top and bottom cell in tandem are currently in research. The most currently used material for a bottom cell are c-Si and CIGS. Silicon exhibits a number of characteristics that a bottom cell in a tandem, or two-cell multi-junction, requires. It has a near-ideal bandgap (Eg = 1.12 eV) for optimal tandem performance and is also relatively cheap for modules. In the case of c-Si, research is underway to enhance the infrared response and reduce Ohmic losses in the cell, which could lead to new processes and cell architectures that could be scaled up and incorporated into modules. CIGS provides an additional advantage as bandgap tuning is possible by changing the chemical composition.

As a top cell, most commonly used materials are III/V, CIGS/CdTe and Perovskite. In the high band gap level of tandem, CIGS does not seem to be a suitable absorber material. Due to the prospect of changing the band gap by tuning the chemical structure, a semi-transparent form of CdTe could be more promising [85]. Due to some advantageous features of perovskite, it may

prove in the future as one of the best material to be used as a top cell in tandem devices.

The thesis is focused on 4T tandem devices having perovskite as the top layer and silicon as a bottom layer.

1.3. Perovskite solar cells

1.3.1. Structure and material property

Perovskite solar cells consists of organic-inorganic hybrid materials which have sparked a strong interest among scientists all over the world. It is a semiconductor that follows a general chemical formula ABX_3 as shown in Figure 1.6. The structure shown in the figure below has A and B as cations while X is an anion.

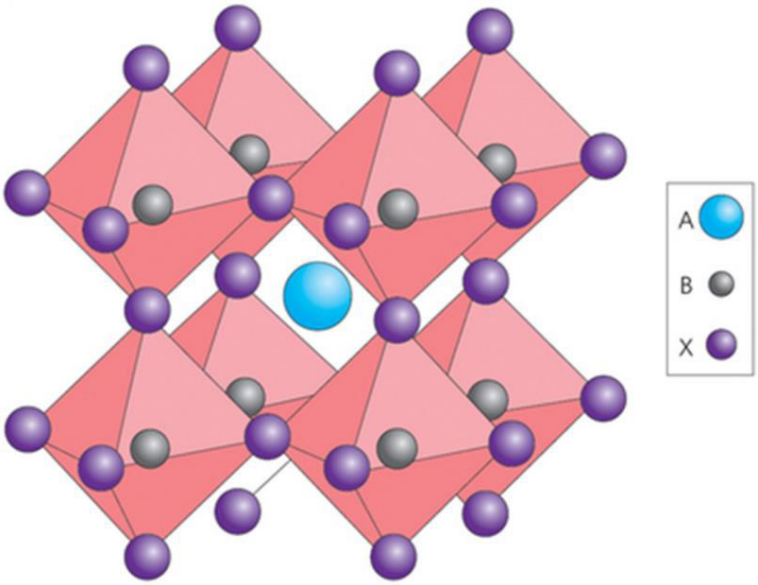

Figure 1.6: Crystal structure of Perovskite

Methylammonium (MA) $CH_3NH_3^+$ or Formamidinium (FA) $CH(NH_2)_2^+$ or Caesium Cs+ or combination of any of these is used as a cation, represented as A in the crystal structure. Pb(II) or Sn(II) or combination of both is used as a metal cation expressed as B and X represents halide such as Cl^-, Br^- or I^- [39]. Perovskites are ideal for a variety of applications due to their highly tunable nature and unique relationship between structure and property. The use of smaller bromide(Br) as a substitute for iodide(I) at the X site can result in efficient bandgap tuning of MA related perovskites between 1.5 and 2.3 ev [54].

Lead halide perovskites are perhaps the most highly studied perovskites for solar cells. Because of their exceptional optoelectronic properties, they are the most efficient among other materials. Also, because of their direct optical bandgap, they are gaining significance as a material for solar cells, as well as for LEDs, and photodetectors [13],[85],[20].

In the visible spectral region, perovskites have high absorption coefficients of the order of 10^5 cm^{-1}[28],[8],[79],[80]. As a result, few hundred nanometers of perovskite layer is sufficient to absorb the majority of incident light. These thin layers are advantageous for effective extraction of photo generated charge carriers, in addition to reducing the material costs[28]. Perovskites also have sharp absorption edges, resulting in low Urbach energies of about 15 meV, similar to GaAs, a direct bandgap crystalline semiconductor with excellent opto-electrical properties [18].

1.3.2. Challenges

Despite the fact that perovskite solar cells are approaching the market leader silicon in terms of performance, the cost of silicon solar panels has fallen so dramatically due to the growth and maturation of manufacturing methods that cheap material costs of perovskites are no longer a strong marketing tool for the technology.

Toxicity: A structural failure in the solar panel may cause problems that endanger the environment. The degradation of PSCs can be induced by exposing them to the ambient conditions. Lead(Pb) is the key component in almost all high-performance PSCs produced nowadays. Pb is considered a toxic constituent because of their environmental and public health toxicity. Lead(Pb) can be absorbed by the skin, the lungs, and the gastrointestinal tract. It can be transported by blood to soft tissues in the human body.

The use of Sn(tin) in place of Pb in PSC may be considered as an option in future because Sn based perovskite solar cells are likely to have high PCE, but the device has very poor stability as compared to the Pb based PSCs [81]. Thus unless the PCE and stability are overcome, or other hybrid perovskite solar cells are developed, Pb based perovskite solar cells will be the standard. Therefore it is important that necessary precaution must be taken to ensure adequate processing and recycling of perovskite solar cells in order to reduce their effects on the environment.

Stability issue: Even though PSC has extraordinary features and outstanding efficiency (in lab), the possibility of commercialization have been hampered due to their long-term instability. Perovskite solar cell degrades at high temperatures and also in humid atmosphere because of the organic entities in the material and their hygroscopic nature[19],[16].

Hysteresis: When solar cells are subjected to the standard AM 1.5G spectral illumination, the current vs voltage (I-V) characteristics are used to analyze the efficiency. A voltage sweep is used to measure the current generated by the cell at various voltages. In perovskite solar cells, the amount of current produced for the same voltage varies depending on the direction and speed of the voltage sweep.

The disparity in the J-V curve generated by sweeping the voltage in the forward direction i.e. from a negative to a positive value and in the reverse direction i.e. from a positive to a negative value is referred to as hysteresis. It may lead to incorrect reporting of different parameters of the solar cell such as power conversion efficiency (PCE)[35]. Thus, a steady-state PCE monitored at mpp over a certain time is now commonly used and approved by the perovskite group for a more reliable evaluation of solar cell results.

1.4. Outline

The structure of the report is as follows and the report is divided into 7 chapters.

Chapter 2 will present the overview of the complete study with literature review of the topic having objectives and research question for the study. In Chapter 3, the methodology to perform J-V measurement and conducting Suns-Voc test for perovskite solar cells/module will be explained with flowchart. Chapter 4 will discuss the characterization of perovskite solar cells/modules using Suns-Voc method. This chapter involves the discussion about the validity of superposition principle for perovskite devices. Subsequently in Chapter 5, the temperature dependency of the various electrical parameters of the perovskite module will be observed. Calculation of temperature coefficients for open circuit voltage ($k_{th\text{-}V_{oc}}$), short circuit current density ($k_{th\text{-}J_{sc}}$) and maximum power($k_{th\text{-}P_{PCE}}$) is done. In the next chapter i.e. in Chapter 6, an alternative measurement protocol for perovskite devices has been practiced. The validity and the necessary requirements for the protocol has been explained further in this chapter. Finally, the conclusions made based on three different study as explained in Chapter 4, Chapter 5 and Chapter 6 are presented in Chapter 7. Lastly, the relevant extra information are included to the appendices.

2

Literature Overview

This chapter aimed at presenting the overview of the research while discussing the literature. Section 2.1 starts with the introduction of the study and describes the state of the art of PSCs and other solar cells. In Section 2.2, the literature review of Suns-Voc method is explained along with the fundamentals of the method. The review of superposition principle is also discussed in subsection 2.2.1 since the Suns-Voc method uses the principle for the analysis. Thereafter in section 2.3, the behaviour of PSCs with temperature dependence as found in literature is explained. In section 2.4, the methods used to track MPP for PSCs is discussed. Lastly, in section 2.5, the overall objectives of the study along with research questions is presented in this part.

2.1. Introduction

A PCE of 25.5% has been achieved for a single junction PSC (perovskite solar cells) in the laboratory. Generally, PCE of a solar cell in lab is computed at STC, which is different than the conditions in field. Solar cells at outdoors operate at varying temperatures and light intensities, resulting in variations in the average PCE. The effects of these outdoor operating circumstances have received little attention in the field of PSCs. Some past studies have used PSCs/modules that were kept outside. However, at the present state of research of PSCs, more structured and complete studies are necessary before conducting tests on large scale at outdoor locations. Thus, operating in a laboratory setting may be preferable, which allows for far more consistent and systematic data gathering while avoiding parasitic failure mechanisms caused by inadequate encapsulation or other unanticipated situations. All aspects discussed in this chapter is relevant to understand the fundamentals and behavior of PSCs while operating under real world conditions.

The performance of a solar cell depends on parameters such as : Short circuit current density (Jsc), Open circuit voltage(Voc) and Fill Factor (FF). For attaining maximum efficiency, these parameters should be optimized.

Different models are used to calculate the maximum PCE of a solar cell. Detailed balance (DB) efficiency method according to the Shockley-Queisser model is most commonly used to calculate and predict the maximum possible PCE of solar cell. The maximum theoretical PCE limit of the PSC is around 31% and it approaches to the SQ limit i.e. 33.5% for single junction solar cell under STC [72]. Owen D. Miller and others has shown that GaAs has attained the theoretical efficiency limit of 33.5% (SQ limit) [53]. According to the SQ model, the calculation of efficiency limit is based on the radiative recombination and the effect of Auger recombination has not been considered.

The fundamental DB (detailed balance) limit of the PCE and the comparison of the maximum PCE of different materials is shown in Figure 2.1 [50]. The record maximum efficiency of PSC is 25.5% for very small area [37].

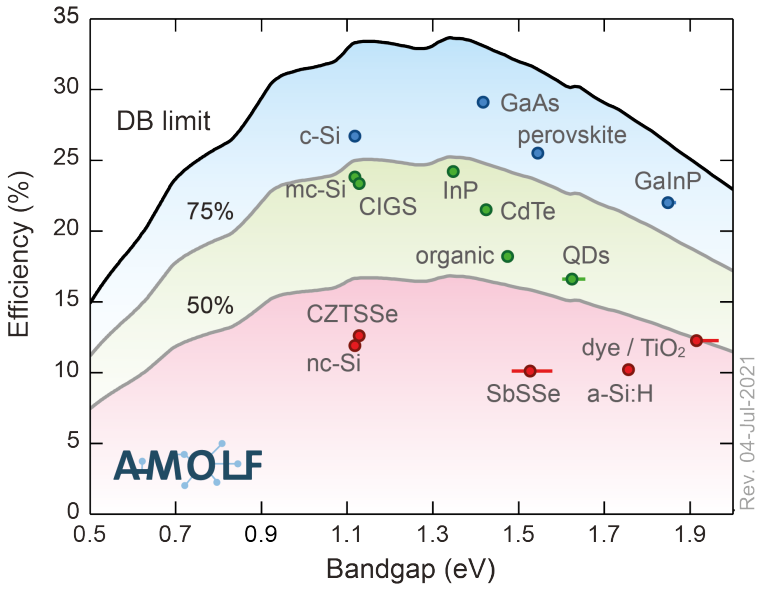

Figure 2.1: Record efficiency relative to detailed balance limit [50]

An important feature to attain high PCE of PSCs is Voc deficit. Voc deficit is described as the difference between bandgap voltage and Voc. The equation of the V_{oc} deficit is given by:

$$V_{oc}deficit = \frac{E_g}{q} - V_{oc} \tag{2.1}$$

where E_g is optical bandgap, q is charge and V_{oc} is open circuit voltage

As shown in Figure 2.2, the Voc deficit of the best PSC is approximately 0.37V which is close to CIGS (0.38V), much smaller than the Voc deficit of organic solar cell (0.6V) and also smaller than the Voc deficit of inorganic c-Si solar cell (0.44V) [88].The non-radiative recombination of the photogenerated charge carriers is determined by the Voc, which indicates that higher V_{oc} means lower non-radiative recombination. Thus, small Voc deficit of PSC may lead to better light absorption and give PSCs a large open circuit voltage.

However, FF of PSCs on the other hand underperforms in comparison to the outstanding Voc. The FF of the best PSC is 83.2% as shown in Figure 2.2 which shows the comparison of FF of various devices with best performance. The FF of PSC is lower than that of GaAs (86.7%) [41] and also lower than the maximum FF of monocrystalline Si (84.9%) [94], even though PSC has wider bandgap and comparable Voc deficit. Thus, it is important to understand and reduce the FF losses for achieving better performance of PSC.

Recombination and series resistance (Rs) at maximum power point (MPP) are the dominant factors for limiting the FF of a solar cell in absence of shunts. Also the ideality factor of a solar cell has an impact which limits the FF. As discussed earlier, the small Voc deficit in PSC suggests that non radiative recombination is not the major cause of the FF loss considering that recombination at maximum power point is not vastly different from recombination at Voc. Thus, Rs in the solar cell is a large factor contributing to the FF loss.

Kim et al. [33] reported the limiting factors in FF characterizing J-V parameters of PSC with different thickness of HTL(Hole Transport Layer). It was found out that when HTL thickness is decreased from 310 nm to 130 nm, various parameters such as Jsc, Voc, ideality factor (n) and Rsh (shunt resistance) does not change while Rs falls monotonically. This decrease in Rs improved the FF of PSC from 72% to around 77%. The calculation of FF was done using an expression as

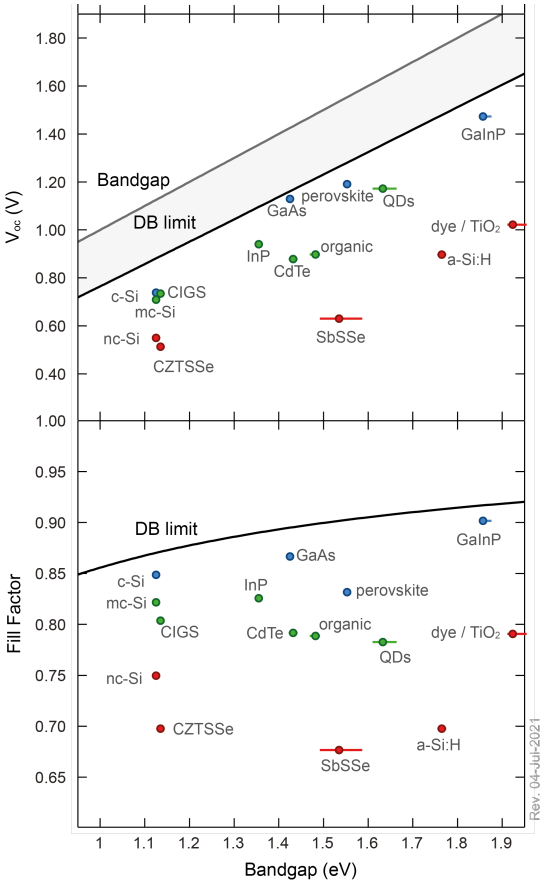

Figure 2.2: Voc deficit and FF for all best efficiency devices [50]

given below :

$$FF = FF_s(1 - \frac{v_{oc} + 0.7}{v_{oc}} \frac{FF_s}{r_{sh}}) \tag{2.2}$$

where

$$FF_s = FF_0(1 - 1.1r_s) + \frac{r_s^2}{5.4} \tag{2.3}$$

$v_{oc} = qV_{oc}/nk_BT$, r_s and r_{sh} are normalized resistance.

$r_s = J_{sc}R_s/V_{oc}$, $r_{sh} = J_{sc}R_{sh}/V_{oc}$

Similar results were obtained by Stolterfoht et al. and it was concluded that the increase in the FF of PSC was due to the reduction in transit time for the carriers as a result of reduced thickness of HTL. As a result, PSC's performance improves [78].

The above studies calculated maximum FF (similar to ideal cell) with negligible Rs and infinite Rsh which was determined by the following equation as shown below :

$$FF_{max} = \frac{v_{oc} - ln(v_{oc} + 0.72)}{v_{oc} + 1} \tag{2.4}$$

The equation used for PSC was initially derived for Si solar cells in low injection operation[31]. This expression has encountered errors upto 6% and 10% for Si solar cells under normal and extreme operating conditions respectively [46]. Also, in all these studies, the Rs is computed

by fitting 1 sun JV curve with diode equation which can result in 6% error. Lastly, Rs was estimated for only one sweep direction in these investigations. Given the hysteresis nature of PSCs, it is crucial to investigate the relationship between Rs and sweep directions i.e. forward and reverse.

Therefore, in order to calculate Rs for PSC which is a limiting factor for FF loss, Suns-Voc method is used for accurate determination of Rs than the fitting of 1 Sun JV curve.

Suns-Voc, however, is presently an indoor experiment under test conditions. Therefore, the influence of real operating parameters like temperature, weather conditions etc needs further study for understanding the performance and degradation mechanisms and, as a result, increasing overall reliability. Moreover, the use of solar cells necessitates long-term operating reliability. One of the major standard experiments for assessing the degradation of developing solar cell (such as PSCs) in lab is exposing the device to prolonged operation at the MPP under one sun illumination and increased temperature. Also, in Suns-Voc measurement, the most important point is MPP on one sun J-V curve. The series resistance computed using the Suns-Voc technique is performed at MPP because it characterizes the optimal working conditions of a solar cell. Thus, it is crucial to have a Maximum Power Point Tracking (MPPT) system that can track the true MPP constantly throughout operation.

2.2. Suns-Voc

The fundamental concept and methodology for the Suns-Voc method, as well as the similar method of Jsc-Voc, were initially defined in 1963 [91] and have been employed in a variety of implementations [64]. Despite its early publication, Suns-Voc was not extensively utilized until a paper was published in 2000 [75] and a commercial instrument became available. Sinton and Cuevas [75] introduced the Suns-Voc method for solar cell characterization, which is presently extensively utilized in the PV community. The Sinton Suns-Voc tool is used for Si solar cells by using a light flash from Xenon lamp. The setup measures Voc and varying light intensity (using a separate calibrated light sensor). The intensity of light varies from few Suns to 0.001 Sun. The Voc at one sun illumination measured from Suns-Voc method should be equal to the Voc of J-V characteristics if the lamp's spectrum is the same. The measuring mechanism can be explained as :

$$J = J_0(exp(\frac{q(V - JR_s)}{nk_BT}) - 1) - Suns.Jsc + \frac{(V - JR_s)}{R_{sh}} \tag{2.5}$$

where J_0 is dark saturation current density, Suns is light intensity, R_{sh} is the shunt resistance, n is the ideality factor [6]. Because the test is being performed in an open circuit condition, the external current density J is equal to zero. Therefore the equation 2.5 can be expressed as :

$$Suns.Jsc = J_0 exp(\frac{qVoc}{nk_BT}) + \frac{V}{R_{sh}} \tag{2.6}$$

Using equation 2.6, a graph between Voc and Suns can be plotted with a given value of Jsc. The Suns-Voc method uses the superposition principle for the analysis of the measurement. Since no current is extracted during the experiment, the data extracted is subsequently utilized to construct a pseudo JV curve and pseudo FF is computed using pseudo JV curve which is free of series resistance. The Voc of a solar cell can be determined before the metallization process since the Rs of the cell has no effect on the voltages measured. This helps in the optimization of operations prior to metallization. The series resistance is calculated by comparing the pseudo JV curve with the 1 sun JV curve at any intensity level (also at MPP).

$$R_{s,\text{Suns-Voc}} = \frac{\Delta V}{J_{mpp}} \tag{2.7}$$

Equation 2.2 is used to calculate Rs at MPP where ΔV is the voltage difference the pseudo J-V curve and one sun JV curve at maximum power point(MPP). J_{mpp} is the short circuit current density

at MPP.

The Suns-Voc method has also been extensively used as one of the technique to characterize inorganic solar cells [65], [17], [40]. The Suns-Voc measurements were also done on high performance kesterite solar cells to understand the problem of non-ohmic back contact and also to observe and reduce the Voc deficit issues [32].

Another research was done experimentally to show that application of Suns-Voc method can be applied on organic solar cells [77]. They were able to compare pseudo-IV curves with the I-V curve obtained under standard conditions to extract series resistance. Also some qualitative information were obtained about recombination processes from the measurement.

As described earlier, the characterization using Suns-Voc method has been performed for testing at cell level. However, in the study done by Alex et al. [44], the technique is used for characterization at module and array level. They also concluded that it can be used to determine the performance, degradation and also to detect problems in the module such as cell cracks, hot spots etc.

2.2.1. Superposition Principle

The commonly used shifting approximation that the current density of an illuminated solar cell is the dark current shifted by the short-circuit photocurrent is derived using the superposition principle.

$$J_L = J_{sc} + J_D \tag{2.8}$$

where J_L is the current density under illumination and J_D is the current density under dark.

It is important to understand the output of a solar cell under operating field conditions. The use of this principle substantially simplifies the estimation of the current and power output from a solar cell at various biases and illumination levels. Thus, the superposition principle is generally assumed to be valid in the analysis of solar cell performance. With information of dark characteristics of a solar cell, equation 2.8 can be used to determine the solar cell performance at any illumination. It considerably simplifies the computation required for analysis and also allows the use of the standard simplified equivalent circuit (Figure 2.3).

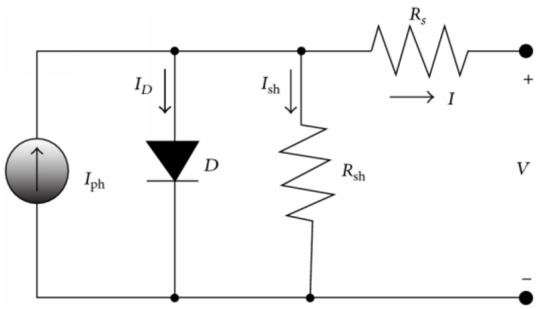

Figure 2.3: Single diode equivalent circuit model of solar cell [93]

The validation of superposition principle (i.e. in absence of series resistance (R_s), the illuminated J-V characteristics is equal to the dark Current density shifted by Jsc) is important to reconstruct the pseudo J-V curve and determine the R_s using Suns-Voc method. The conditions necessary to validate the superposition principle are stated in Section 4.1 of Chapter 4.

Lindholm et al. in the year 1976 examined the validation of the principle of superposition using mathematical analyses [48]. They deduced that the principle holds until the low level of injection of minority carrier concentration is maintained and are not exceeded, the contribution of depletion region is not significant to both the carrier recombination and photogeneration and also the series and shunt resistance effects are negligible. However, the paper published by Tarr and Pulfrey in 1979 said that the superposition principle still holds even if the contribution by the photogeneration and recombination in the depletion region is substantial to the photocurrent and dark current respectively [83].

Also, the validation of superposition principle for Si and GaAs homojunction cells were justified under 1 sun illumination. Later in 2003, experiments were performed on CIGS solar cells to verify the superposition principle. The principle fails for CIGS solar cells and it was the observed that at lower temperatures the failure becomes more distinct [27]. According to the authors, a secondary barrier which results from the conduction band offsets between CdS window layer and CIGS produce a secondary diode that creates a shift in voltage between the light and dark conditions. Furthermore, it was mentioned by A.E. Delahoy and their coworker that the thin film CdTe solar cells also does not follow the superposition principle [2].

Another interesting study was done on perovskite solar cells using experimental and simulated data [66]. The analysis showed that the superposition principle does not hold for the device and they concluded that the photocurrent is indeed bias dependent. In order to reduce bias dependency, they suggested three schemes aimed at improving the performance of the device. Scheme 1 imply doping of the perovskite layer, Scheme 2 involves doping of ETL/HTL layer whereas Scheme 3 investigates the doping of perovskite along with the ETL/HTL doping. Using simulations, they were able to justify that the principle can be validated if appropriate doping of ETL/HTL is done following Scheme 2. An improvement in the performance i.e. increase in FF was observed using the above mentioned method.

2.3. Variation of temperature

A constant source of light intensity has been utilized to lower the prices of solar cells and increasing their PCE. However, the rise in irradiance is associated with temperature increase, which has a negative impact on solar cell performance. Thus, studying the behavior of solar cells under various temperature and irradiance is unavoidable in order to understand and estimate their performances at a given illumination level and temperature, because the operating conditions in reality differ from those of STC.

Several research have been conducted to determine the influence of temperature on the performance of solar cells based on various semiconductor materials. Arora et al.[59] used a computational model in 1982, that took into consideration that physical processes depends on temperature, to explore theoretically the temperature dependency of the Si (silicon) p-n junction solar cell. Later in 1986, Fan [25] calculated the temperature dependency of the electrical characteristics for solar cells made of various materials (Ge, Si, GaAs). It was concluded that when the band gap energy of solar cells is higher, temperature has less effect on their performance. Philipps et al.[58] examined the impact of temperature on the GaAs solar cell theoretically and empirically in 2011. In 2012, Singh et al.[74] examined the performance characteristics of solar cells based on Si, Ge, CdTe, InP, GaAs and CdS materials at various temperatures. Chander et al.[82] studied the impact of temperature on monocrystalline Si solar cell in 2015 and reported that the temperature coefficients of Jsc, Voc, and PCE are +0.2, -0.22, and -0.4%/K, respectively.

In this study, the effect of temperature on the performance of perovskite module was examined. According to preliminary studies on the most fundamental temperature dependency of perovskite solar cells, power conversion efficiency (PCE) is maximum at room temperature, with diminished

performance at either high or low temperatures [51], [21]. J-V measurements show a 2 to 60% rise in the FF across the temperature range of 0°C to 70°C [47],[95]. This increase was observed due to efficient charge collection for elevated temperature till 70°C and then it showed a decreasing trend of FF at temperature higher than 70°C due to high interfacial recombination among the selective contacts .

According to some report, it has been observed that Voc decreases linearly with temperature, which is consistent with other types of solar cells having a negative temperature coefficient [29],[56]. According to the literature, the short circuit current density is hardly impacted by temperature variations below 55°C but considerably reduced at higher temperatures [55].

The influence of temperature cycles on the photovoltaic efficiency of perovskite solar cells was recently examined also with the temperature dependent measurements. Cheacharoen et al. found that there is scarcely any deterioration when the perovskite solar cells were encapsulated and they were cycled between -40 °C to 85 °C while keeping the cells in the dark [11].

2.4. Maximum Power Point (MPP)

The maximum power point (MPP) is a point on a JV curve where the PV device produces the maximum power, i.e. when the product of current density and voltage is maximum. The MPP may fluctuate as a result of environmental influences such as temperature, illumination conditions etc. MPPT can be used to adjust the resistance of a solar PV device in order to ensure P_{max} in the presence of these external variables.

The advancement of solar cell technology necessitates the development of reliable device characterisation methods that produce performance data that is indicative of device functioning in steady state. The most popular approach for evaluating the device performance of solar cells is to utilize J-V measurements. In case of perovskite solar cells, there have been debates highlighting that the results obtained i.e. PCE and MPP from the standard J-V measurements may not be reliable and accurate because of the hysteric behavior of the perovskite solar cells [87], [14]. Maximum power point tracking (MPPT) should be used to evaluate device performance instead of the PCE or MPP derived by J-V measurements, which may become a more important metric for evaluating the performance of PSCs [15],[57].

Maximum power point measurements over time may be done in a variety of ways. To prevent reporting artificial power conversion efficiencies for perovskite solar cells, three techniques have been mostly accepted:

(i) MPPT method [88],[68],[89] - Different MPPT techniques are used such as Perturb and Observe (P&O) method, Incremental Conductance Method, Open circuit voltage method etc. For PSCs, P&O method is generally used as a MPPT algorithm.

(ii) Steady State Power Output approach [54],[76] - In this method, current is measured continuously by keeping the voltage fixed until stabilisation is achieved. If the voltage is properly set to be the V_{mpp}(maximum power point voltage), this measurement results in a steady state efficiency.

(iii) Dynamic J-V measurement [76],[67] - The dynamic J-V measurement is similar to the standard J-V measurement. The waiting period at each step in the voltage applied is not fixed in case of the dynamic J-V technique, but is permitted to change in order to attain a certain degree of stability in the current measured, whereas the waiting time is fixed in case of the conventional J-V measurement.

2.5. Objectives & Research question

Suns-Voc technique has been widely used to characterize different type of solar cells. This method involves measurement of voltage as a function of illumination intensity without extracting current from the device. Because no current is flowing during the experiment, the approach is used to generate pseudo-JV curves that depict the generation and recombination processes without an effect of series resistance or the photoactive layer's transport resistance.

The calculation of series resistance are also commonly done by fitting the one sun J-V characteristics with the diode equation and is prone to errors upto 6% as depicted by Pysch et al. [17] and Kim et al [33].Thus, the Suns-Voc method is used to give a more reliable estimation of series resistance as compared to fitting of one sun J-V curve [17]. The project aims to characterize the perovskite module using the Suns-Voc technique by generating pseudo J-V curve to calculate series resistance of the module.

As the analysis uses the superposition principle, the prior goal of the study is to determine if the concept of superposition holds true for perovskites.

Additionally, the study aims to investigate degradation mechanisms in perovskite module under various light intensities and temperature variations in order to better understand and acquire insight on outdoor device performance. Finally, to track the true optimal power output at MPP, a new protocol has been developed which can be employed in lab. This measurement method can be used for various other devices including perovskite solar cells.

The following key research question will be used to carry out the project's goal :

"How does the top perovskite solar cell in tandem device behave under real operating conditions?"

The following sub questions are defined that will answer the key research question:

(1) What are the constraints on applicability of superposition principle and Suns-Voc method in perovskite solar cell/module as a top cell in tandems ?
(2) How does the perovskite module behave under the influence of different temperature and light intensity ?
(3) How to track the true MPP of the perovskite solar cells/module in laboratory ?

3

CHARACTERIZATION METHODS

This chapter discusses the two characterization methods used in the study. Section 3.1 describes the methodology used to characterize the perovskite device using standard J-V measurement. In Section 3.2, the methodology used to perform the Suns-Voc test is explained. Variations of temperature with irradiance and the MPPT measurement are described in the dedicated chapters.

3.1. J-V Characterization

To address the research questions of this study, the methodology used are illustrated in the Figure 3.1, 3.2 3.3. The methodology has been divided into 3 steps, stabilization, pre-conditioning test and I-V measurement. Figure 3.1 represents the start of the experiment, where the source irradiance of solar simulator is adjusted with the help of calibrated reference Si solar cell. Then, the device is exposed under one sun illumination and hysteresis from the I-V curve is analysed from forward and reverse scan. The standard J-V measurement of thin film solar cells like CIGS, CdTe, a:Si etc requires preconditioning before measurement of J-V characteristics as compared to the measurement of c-Si solar cells. For PSCs, preconditioning is required to stabilize the cell as it generally shows hysteresis. Following equation is used to calculate the hysteresis :

$$H = \frac{P_{\text{max}} - P_{\text{min}}}{P_{\text{average}}} \tag{3.1}$$

If the hysteresis of the perovskite solar cell/module is less than 1%, the I-V test done before can be used further otherwise pre-conditioning of the device is needed.

Figure 3.2 explains the steps of preconditioning done to stabilize the device. The perovskite solar cells are stabilized by keeping under one sun illumination at maximum power point. This step takes approximately 7 minutes to complete. After performing the light soaking test, the device is once again tested at 1 sun to obtain I-V characteristics. From the forward and reverse scan, the hysteresis is calculated again using equation 3.1 and compared with the previous value of hysteresis. Generally, it has been observed that the light soaking test leads to stabilize the device and reduces hysteresis. It is very common to repeat the light soaking one more time to reduce the hysteresis further and reach close to 1%.

If the hysteresis obtained are satisfactory to continue with the measurement, the final step is followed and has been explained by the diagram in Figure 3.3. Light I-V test is executed for the perovskite device following dual sweep i.e. from Isc to Voc and vice versa. Different external parameters are extracted from the I-V curve such as Isc, Voc, FF, Pmax and efficiency.

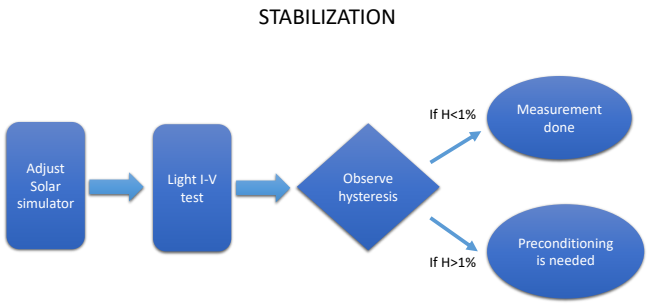

Figure 3.1: Step 1 - Stabilisation

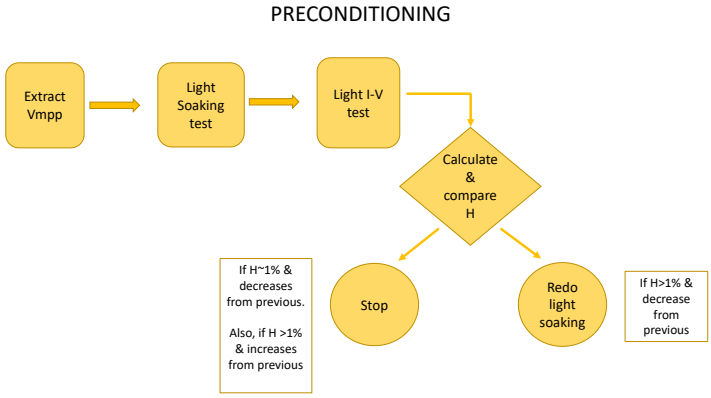

Figure 3.2: Step 2 - Preconditioning

The above processes are the pre-requisite for characterization of perovskite devices and the same procedure has been followed along with other steps as explained later in the following chapters. Also periodic measurements of the perovskite module (area of 100cm^2) has been done to understand the stability of the device.

As it can be seen from the Figure 3.4, the FF and efficiency has remained stable showing consistent result except the measurement done in January. The experiment was performed using WACOM AAA solar simulator and a good relative measurements is sufficient for this study, hence spectral mismatch corrections are not needed at the moment.

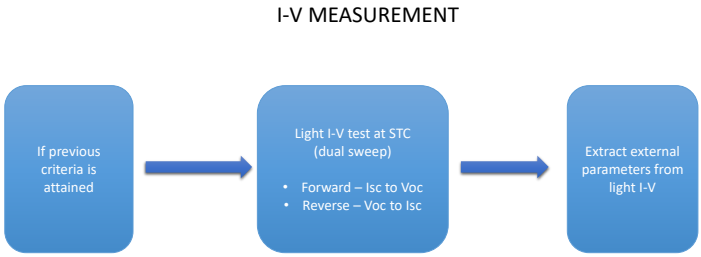

Figure 3.3: Step 3 - Final step to complete the I-V test

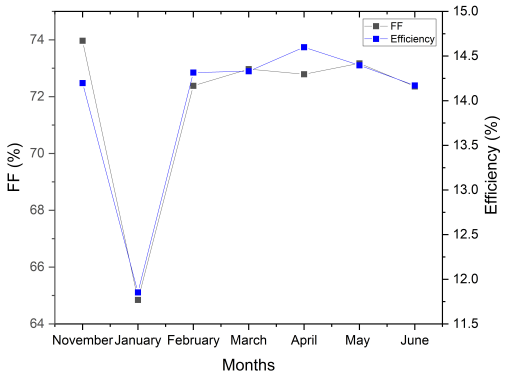

Figure 3.4: Periodic observation of large perovskite module

3.2. Suns-Voc methods

The Sinton tool for Suns-Voc measurement is known for characterizing the Si solar cell by using a light flash from Xenon lamp. It has also been utilized for other solar technologies like kesterites and OPV (Organic photovoltaic) [32],[70] and it could be very useful for PSCs. The complicated behavior of PSC, particularly the well-known high hysteresis restricts the use of the setup because of the short flash decay time. Furthermore, during measurement of other types of solar cells, the built-in Si reference cell in a Sinton setup causes considerable spectrum mismatch, necessitating non-trivial adjustments for reliable results [63].

Here, the J_{sc}-V_{oc} technique is used to characterize perovskite modules and cells which is a precursor of the Suns–V_{oc} method established by Wolf and Rauschenbach [91]. Figure 3.5 shows the methodology used to perform the experiment.
Measurement starts with the adjustment of irradiance of the solar simulator followed by the preconditioning of the PSCs. After preconditioning, standard J-V measurement is done and gray filter is used to vary the illumination from 1 Sun to 0.01 Sun. At each irradiance level, J_{sc} and V_{oc} are extracted by sweeping J-V curve for both directions (forward and reverse). The J_{sc}-V_{oc} pairs are used to construct pseudo J-V with the help of Equation 3.2.

$$J_{\text{pseudo}} = J_{sc}(1sun) \times (1 - \frac{J_{\text{gray filtered}}}{J_{sc}(1sun)}) \tag{3.2}$$

J_{sc}(1 sun) is the J_{sc} obtained under STC and $J_{\text{gray filtered}}$ is the short circuit density calculated at

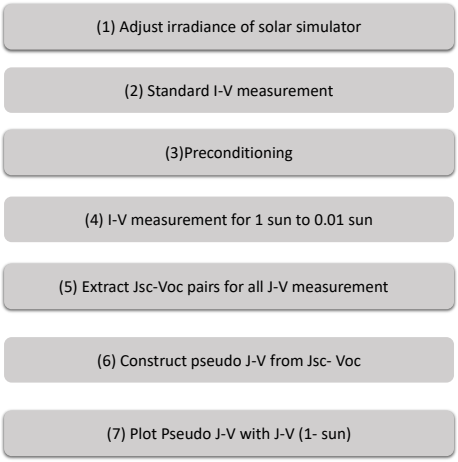

Figure 3.5: Methodology of Suns-V_{oc} (J_{sc}-V_{oc}) test

each reduced illumination level. The temperature is assumed to be constant at 25°C which is a requirement to have consistent V_{oc} measurements at each illumination level. Three different kind of perovskite samples are used for this measurement i.e large module, mini module and pixel cell with active area of 100 cm^2, 3.7cm^2 and 0.18cm^2 respective to calculate J_{sc}.

4

Characterization Using Suns-Voc Method

The characterization of PSC is essential for understanding performance and degradation mechanisms under operating field conditions, which will lead to improved overall reliability and lifetime. The Suns-Voc technique can be a useful tool for gathering data required to understand how degradation and light intensity (different weather conditions) affect various PV designs. This chapter aims to answer the first sub-question introduced in sub-chapter 2.5 which were ”What are the constraints on applicability of superposition principle and Suns-Voc on perovskite solar cells?”. In this chapter superposition principle is explained from the literature in sub-chapter 4.1. Subsequently in sub-chapter 4.2, the steps taken for the experimental to do the measurement is described along with the setup. Later on, the results of the experiment are analysed in sub-chapter 4.3 and finally the chapter is concluded in sub-chapter 4.4 by answering the RQ1.

4.1. Superposition principle

According to the principle of superposition, the total current of a solar cell flowing in an illuminated device is the superposition of the short circuit and the dark (non-illuminated) current at bias voltage.It is also referred as ”shifting approximation”. The solar cell terminal current under light(J_{Tot}) and the dark(J_{Dark}) conditions are related to the superposition principle. The classical definition of the principle at a given carrier generation rate(G) and applied bias is given by :

$$J_{\text{Total}}(G,V) = J_{\text{photo}}(G) - J_{\text{inj}}(V) \tag{4.1}$$

where J_{photo}(G) = Generation dependent photocurrent and J_{inj}(V) = Voltage dependent diode injection current

The photocurrent is assumed to be independent of voltage and also expressed as J_{SC}. The diode injection current is assumed to be independent of generation rate and thus it is approximated as J_{Dark}. Thus, the superposition principle can be represented as :

$$J_{\text{Total}} = J_{\text{SC}} - J_{\text{Dark}}(V) \tag{4.2}$$

The seperation of J_{Total} into J_{SC} and J_{Dark}(V) components is advantageous because it simplifies the challenge of characterizing an illuminated cell connected to any load into two smaller problems: describing J_{SC} of an illuminated cell connected to no load and describing the J_{Dark}(V) of a non-illuminated cell under applied forward voltage.

The superposition principle as per equation 4.2, states that if a system is linear then the response to various excitations will be the sum of responses to each excitation applied alone [24]. Thus, the principle applies only if the necessary boundary value problems shows linearity. This expression (4.2) is true under the following requirements as given by Lindholm et al [24]. The principle was applied to a p-n junction solar cell and conditions were verified using numerical derivations. The conditions required to validate the superposition principle are:

1. The junction space charge area may contribute significantly in either the dark current or photo current.
2. In the quasi-neutral regions, carrier concentrations must remain in low-injection levels.
3. The series and shunt resistances must have a negligible impact on the current-voltage characteristics of the cell.
4. The material properties, such as the lifetimes of minority carriers, must be substantially independent of the illumination level.
5. As the cell is loaded (and the terminal voltage V varies), the volume of the photocurrent-producing areas must stay constant.

There are instances where superposition principle is not valid for solar cells. As stated previously in the literature, solar cells with significant Rs(series resistance) are perhaps the most notable example for the failure of superposition [24]. Due to the presence of Rs, the boundary condition at the edge of the depletion region of the quasi neutral region is effected which results in non linearity conditions and thus prohibit the use of superposition.

The basic assumption in the equation (4.1) is that the diode injection current under illumination is generation independent and equal to the contact injection current in the dark conditions. When the minority carrier lifetime and mobility are low, this approach fails in solar cells [62], [84]. The rate of total recombination can be increased to the point where the actual illuminated J-V characteristics change substantially from those predicted by equation(4.2) if the carrier lifetimes and mobilities are sufficiently small. The effect was illustrated by N.G Tarr and D.L Pulfrey[84] for GaAs cell having short carrier lifetime and low mobility which can be found in poor quality poly-crystalline substrates.

4.2. Experimental Method

A common approach for characterization of solar cells is done by measuring JV parameters under Standard Test Conditions (AM 1.5G, 1000 W/m^2 and 25°C) adhering to the IEC 60904 standard. The electrical and photovoltaic properties of the solar cell are calculated from the J-V characteristics. When the working circumstances such as light intensity, wavelength, temperature are incidentally altered while the parameters of importance i.e. Isc, Voc, FF, etc. are investigated, most of the essential solar cell features are presented. This method helps to study the superposition principle for different solar cells.

A solar simulator is used here as a tool to characterize the perovskite solar cell or module. The solar simulator emits light that is similar to natural sunlight and it creates a controllable indoor testing facility that can be used to test perovskite solar cells/modules under laboratory conditions. A Wacom (AAA Solar simulator) and a Keithley 2400 calibrated source meter is used to characterize the solar cell and module, and to vary the illumination intensity different gray filters are used. Figure 4.1 shows the working area of the solar simulator used in the experiment.

Bi-directional voltage sweeps are particularly important in perovskite solar cells, where high hysteresis in performance is frequently observed and is also expected. Maximum power (point) current (I_{mpp}), maximum power (point) voltage(V_{mpp}), open circuit voltage (V_{oc}), short circuit current density(J_{sc}), fill factor(FF) etc. are all determined from J-V characterization of the cell.

After calibration of the solar simulator using a Si reference cell and adjusting the irradiation intensity, the perovskite cell/module is preconditioned for some period before taking the IV measurement to stabilize and obtain higher efficiency with low hysteresis.

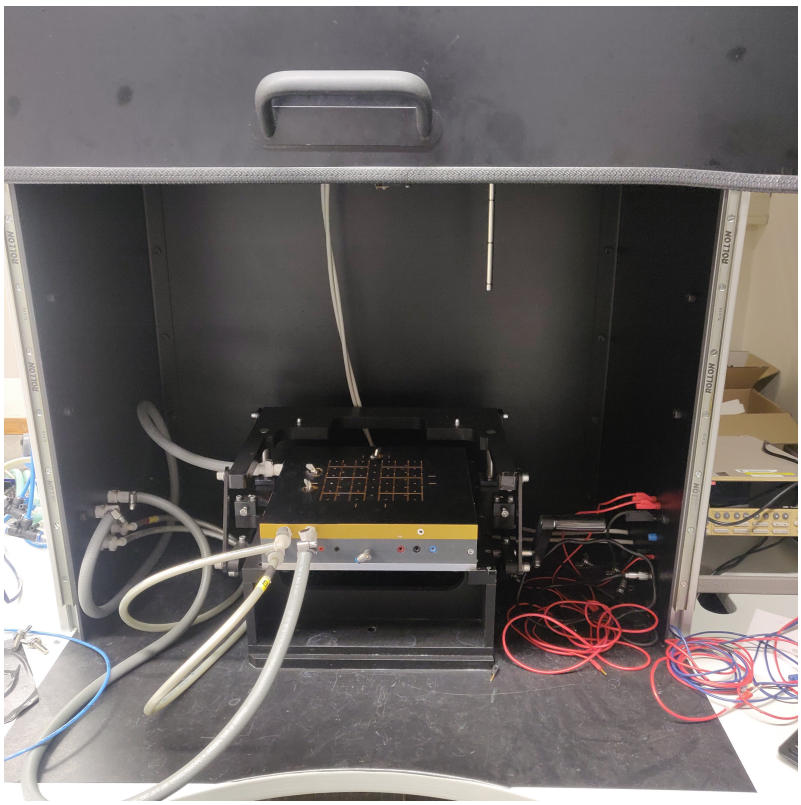

Figure 4.1: Working area of Solar Simulator (WACOM)

The J-V characteristics of the module/cell is first measured without illumination i.e. under dark conditions to generate dark J-V curve. Thereafter, the perovskite module is illuminated under STC and the J-V curve is obtained. Then, different gray filters are used to characterize solar cells at decreasing irradiance and J-V curve is recorded at each illumination level. By sweeping full J-V curve at each level, J_{sc} and V_{oc} can be obtained. Other parameters such as FF, P_{max}, efficiency etc. can also be calculated from each of the J-V curve. The methodology to perform Suns-Voc test is discussed in detail in subsection 3.2 of Chapter 3.

4.3. Experimental Results and Discussion

As described above, a solar simulator(WACOM) was used to characterize the tandem module and Keithley 2400 source measure unit was used to set the test conditions to measure the current voltage characteristics. Perovskite solar cells are illuminated which will generate photocurrent. The important parameters extracted from the I-V curve are open circuit voltage(Voc), which is the voltage at zero current and short circuit current (Isc) which is the current at zero bias. The third parameter is FF (fill factor) which is the metric for the quality of solar cell. It is calculated as the ratio of the maximum power to the product of open circuit voltage (Voc) and short circuit current(Isc). Efficiency can also be obtained from the results extracted above and is given by the ratio of the maximum power produced to the incident power. Efficiency can be computed out as follows :

$$Efficiency = \frac{Pmax}{Pirradiation} = \frac{max(V * I)}{1000W/m^2} = \frac{Voc * Isc * FF}{Area * 1000W/m^2} \tag{4.3}$$

In this project, three different kind of perovskite samples were taken for the experiment fabricated by TNO Eindhoven partner in Solliance. Perovskite module with size of 100cm^2 and 4 cm^2 and a perovskite solar cell with an area of approximately 18mm^2 were used during this project. It is important to note that the J-V measurement should take place after the efficiency has stabilized. Preconditioning is done to stabilize which changes the physical properties of perovskite. A small effect is also observed while doing short measurements. Thus performing a sequence of short measurements without prior preconditioning would deliver a series of measurements on physically different sample and the results would vary for such measurements. Therefore, the solar modules/cells were preconditioned by placing them under illumination for a certain period of time. The time required for stabilization can differ for different device architectures.

The conditions mentioned in section 4.1 lay the basic framework for validation of superposition principle. Of these, the effect of series and shunt resistances on the performance of the various samples can be observed with help of dark and light JV curves.

Figures shown below are the J-V curves under 1 sun illumination and dark conditions for the large module, mini module and the pixel cell. The curves were obtained by sweeping the voltage from reverse bias to forward bias and then to check for any short term instability, go back to reverse bias. Large perovskite module were sweeped between 35V to -0.1V with 101 steps and between 7V to -0.1V and 1.2V to -0.1V for perovskite module of 4cm^2 and perovskite solar cell of 18mm^2 respectively with the same number of steps to obtain the full I-V curve.

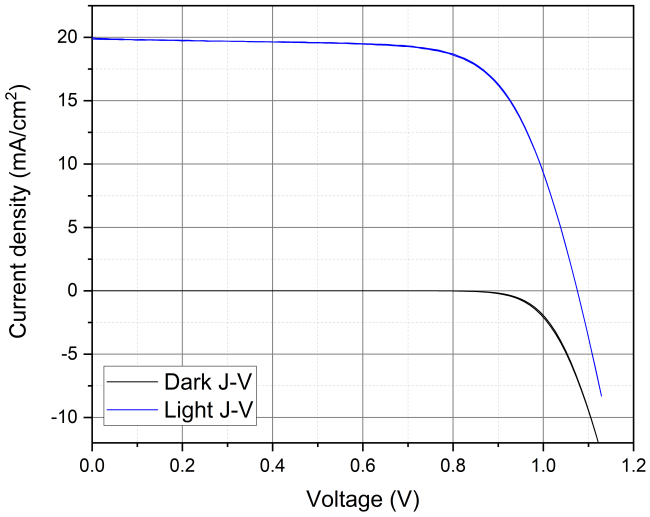

Figure 4.2: Light J-V vs Dark J-V for large module

Direction	Active area(cm^2)	Jsc(mA/cm^2)	Voc(V)	FF(%)	Efficiency(%)
Forward	92.5	19.75	1.07	72.36	14.17
Reverse	92.5	19.60	1.07	73.42	14.28

Table 4.1: JV parameters of large perovskite module

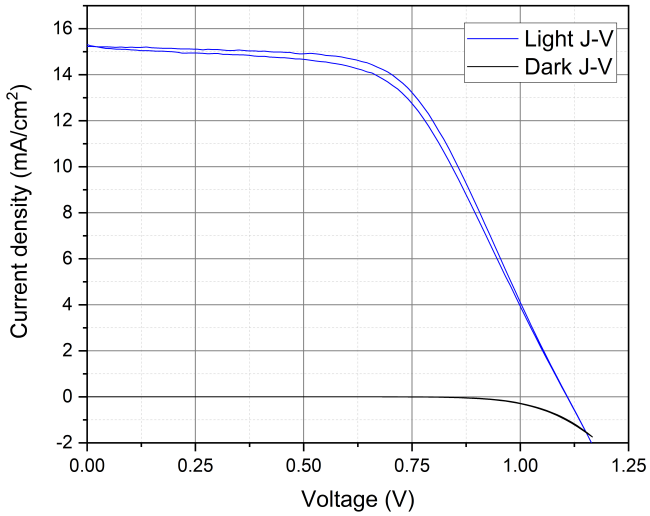

Figure 4.3: Light J-V vs Dark J-V for mini module

Direction	Active area(cm^2)	Jsc(mA/cm^2)	Voc(V)	FF(%)	Efficiency(%)
Forward	3.7	15.21	1.108	56.71	8.847
Reverse	3.7	15.21	1.109	58.79	9.179

Table 4.2: JV parameters of perovskite mini module

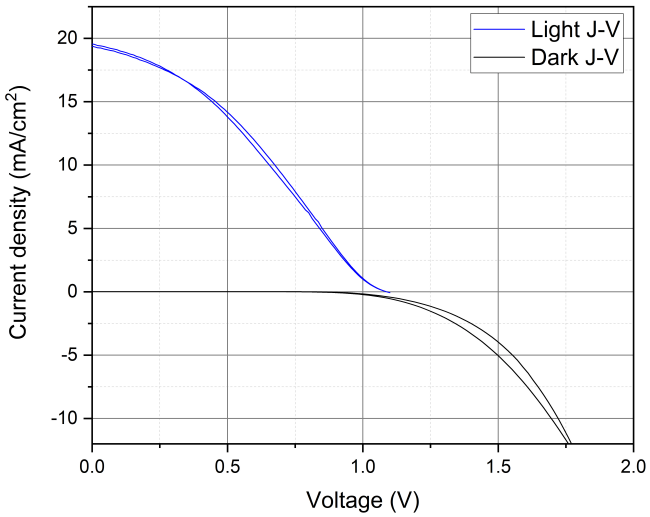

Figure 4.4: Light J-V vs Dark J-V for perovskite solar cell

As the devices are scanned in forward and reverse direction, the J-V curves are subject to hysteresis which cause different MPP's. MPP refers to the point on the J-V curve where the device produces maximum power. As discussed before, hysteresis is determined using Equation 3.1 from J-V curve sweeped in both direction. Based on the measurement, our sample has hysteresis of about 0.8%, 3.7% and 3.81% for large module, mini module and pixel cell respectively. Also a

Direction	Active area(cm^2)	Jsc(mA/cm^2)	Voc(V)	FF(%)	Efficiency(%)
Forward	0.18	19.33	1.077	36.37	7.662
Reverse	0.18	19.5	1.08	34.62	7.295

Table 4.3: JV parameters of perovskite solar cell

number of parameters were extracted from the J-V curve and are represented in Table 4.1, Table 4.2 and Table 4.3 for different samples of perovskite.

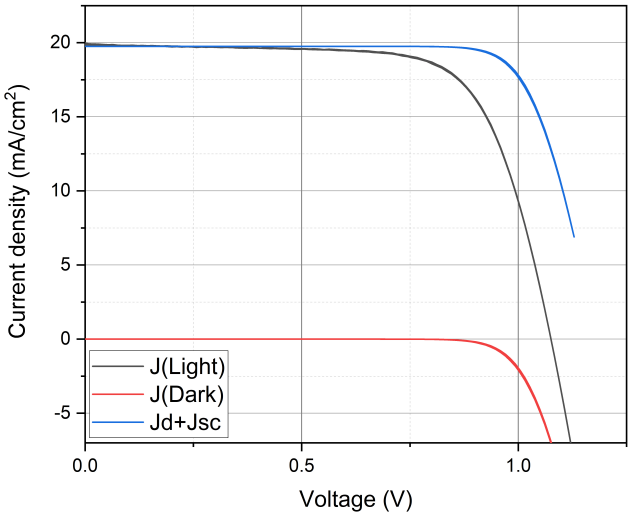

Figure 4.5: Calculated light J-V, dark J-V and Jsc shifted dark J-V of large module (Both scan direction)- Verification of Superposition principle (Method 1)

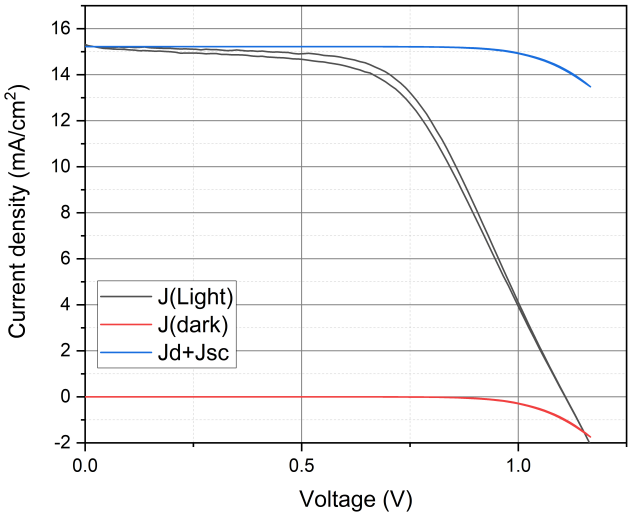

Figure 4.6: Calculated light J-V, dark J-V and Jsc shifted dark J-V of mini module- Verification of Superposition principle (Method 1)

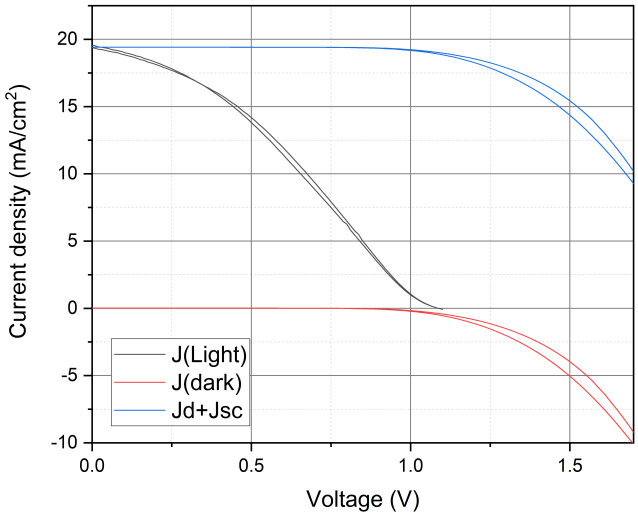

Figure 4.7: Calculated light J-V, dark J-V and Jsc shifted dark J-V of Pixel cell- Verification of Superposition principle (Method 1)

From literature, it is seen that for solar cells, superposition principle is valid when the dark J-V curve shifted by J_{sc} is coincident on the light J-V curve provided the effect of series resistance is negligible. This is tested for the large module, mini-module and pixel cell as shown in Figures 4.5,4.6 and 4.7 respectively. It can be viewed from the figures shown above that the principle of superposition does not hold for perovskite modules and PSC, an alternate method is tested again to validate the principle by varying the irradiation and observing the behavior at intermediate light intensities. Different sets of J-V curves were obtained for each reduced illumination level from 1 Sun to 0.01 Sun and external parameters were calculated such as J_{sc}, V_{oc}, FF, P_{mpp} from the curve. In order to verify the validity of the superposition principle, the dark J-V curve was compared with J_{sc}-V_{oc} pairs obtained with different illumination level [69]. Figure 4.8, 4.9 and 4.10 shows the comparison of dark J-V curve with the J_{sc}-V_{cc} pair for all of the samples.

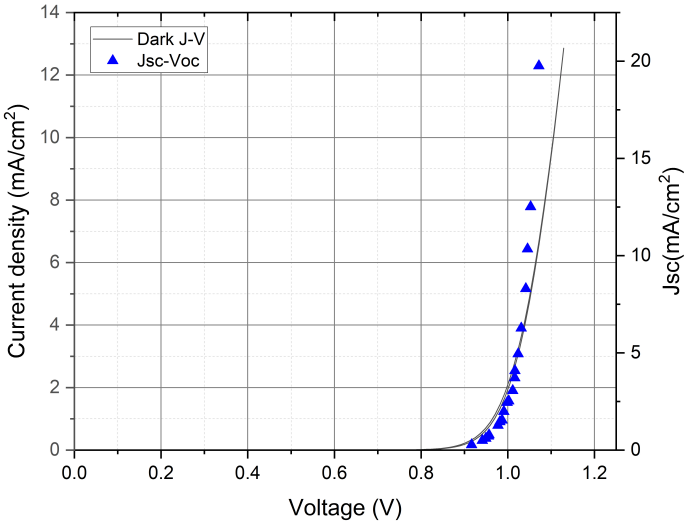

Figure 4.8: Jsc-Voc with calculated dark J-V -Verification of superposition principle for perovskite large module (Method 2)

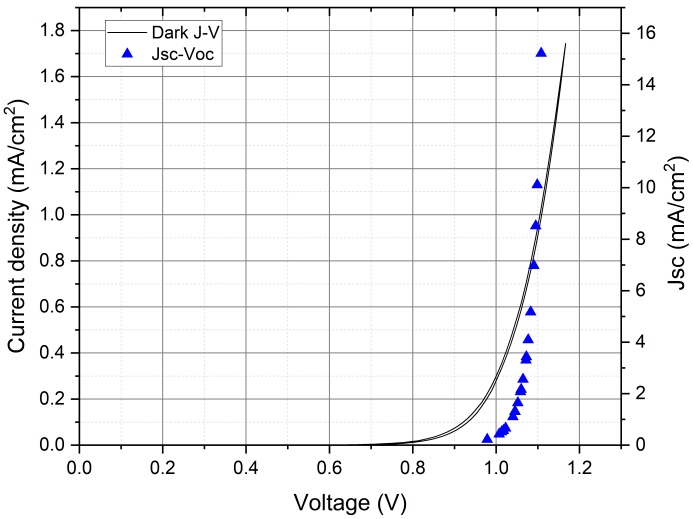

Figure 4.9: Jsc-Voc with calculated dark J-V - Verification of superposition principle for perovskite mini module (Method 2)

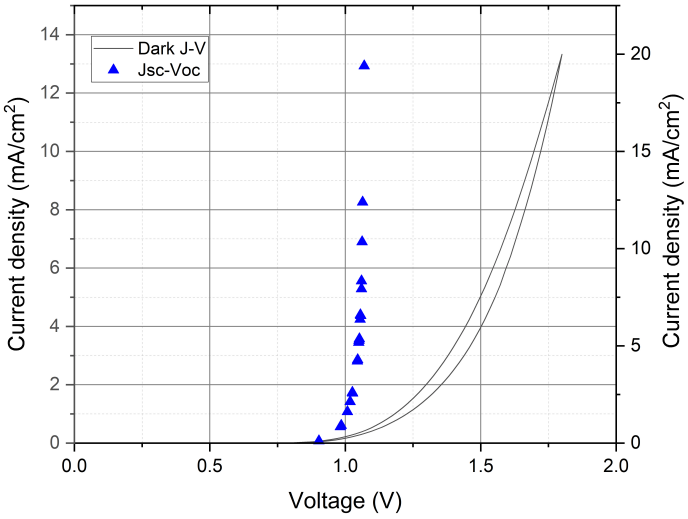

Figure 4.10: Jsc-Voc with calculated dark J-V -Verification of superposition principle for perovskite solar cell (Method 2)

For the large module in Figures 4.5 and 4.8 it is seen that both methods show adherence to superposition principle until certain voltage levels. For Figure 4.5, it is seen that the Jsc-shifted curve is coincident with light JV curve at low voltages. In Figure 4.8, it is seen that the two curves are coincident for data points at low to intermediate light intensities. At higher voltages (and light intensities) a drop in achievable Jsc is seen which is positively increasing with voltage or intensity. The behavior in both cases point towards the increasing effect of series resistance. While it is understood that series resistance is existent, its effect can be neglected if the rate of recombination that leads to resistance is proportional for dark and light curves, thus allowing the coincidence of light and Jsc-shifted curves. The increasing gap is possibly due to the growing influence of non-radiative recombination, like SRH. This phenomenon would explain the decrease in Voc with increase in intensity.

Similarly for the pixel cell, the Figures 4.7 and 4.10 depict the attempt at validating superposition principle. The result shows huge deviation of Jsc-Voc from the dark J-V curves. The pixel cell were not encapsulated and were kept open in air for a long time which could result in degradation of a cell. From both cases, it is evident that there is a significant dominance of series resistance, which can originate from recombination at bulk/interfaces or structural changes in the perovskite layer. Between the large module and pixel cell, the impact of series resistance is larger in the latter. This could be due to possible reasons like: i) Larger active area for the module, which increases carrier availability ii) Presence of carrier collection enhancers in module (metal pins, bars).

The mini-modules showed a different trend between Figures 4.6 and 4.9. While from Figure 4.6 it can be seen that the superposition principle is not valid even at intermediate voltages, the result in Figure 4.9 is interesting where at lower intensities the voltage is higher than the voltage at Dark. This is reversed with increasing intensity, with voltage at dark being higher than measured voltage at 1 Sun. While the latter is usually a consequence of increased bulk recombination, the former needs more understanding and is suspected to be due to the dominant role of surface recombination.

Also as discussed in section 4.1, the classical definition of superposition principle states that J_{photo} is voltage independent and J_{inj} is generation independent. It has been proven before by Raghu Vamsi and others (2015) [10] that the principle is not valid for p-i-n solar cells and a-Si/c-Si heterojunction solar cell as the J_{photo} calculated using the frozen potential approach is strongly bias dependent. Also J_{inj} was found out to have strong generation dependence. The same reason was concluded (bias dependency of the photocurrent) for the failure of superposition principle by conducting a simulation analysis on perovskite solar cell [66]. The equilibrium band diagram as shown in Figure 4.11 from the study [66] shows that till the point where applied bias is equal to the built in potential, efficient collection of charge carriers is observed. The high band offsets at the junction (Perovskite/HTL and ETL/Perovksite) behaves as close to ideal blocking contacts. When applied bias becomes more than the built in potential, the electric field in the perovskite becomes unfavorable for photogenerated charge carriers at the desired contacts of the device. Thus, using past observation, it can be said that the bias dependency of the photogenerated carriers may be one of the reasons for the failure of the principle.

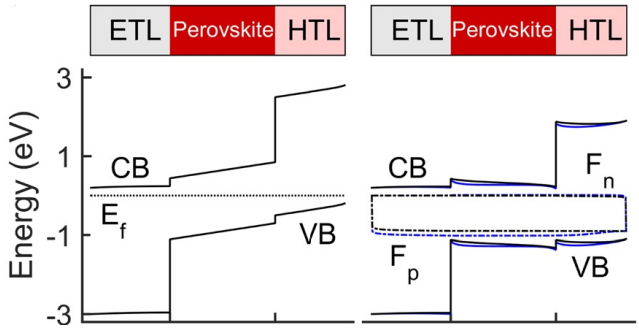

Figure 4.11: Energy band diagram at thermodynamic equilibrium(left panel) and at 0.9V(right panel) [66]

After illuminating the perovskite at 1 sun and under dark, the perovskite modules were exposed to different illumination intensity using gray filters which reduces the illumination level. The J_{sc}-V_{oc} points were extracted at each reduced illumination level by sweeping the full J-V curve in both forward and backward direction.

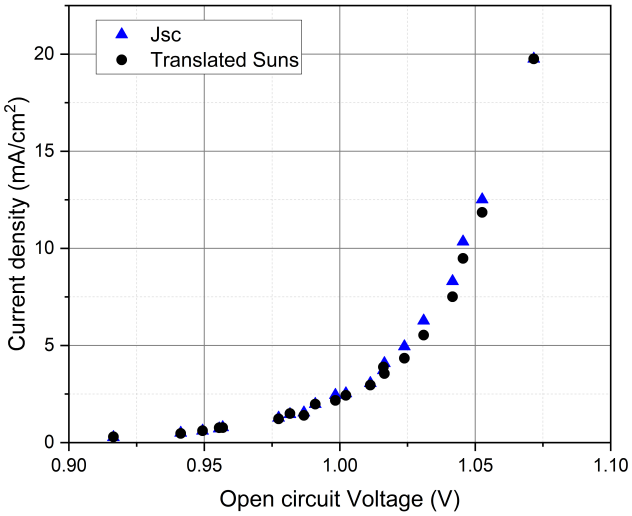

Figure 4.12: Effect of light intensity on Jsc of large module

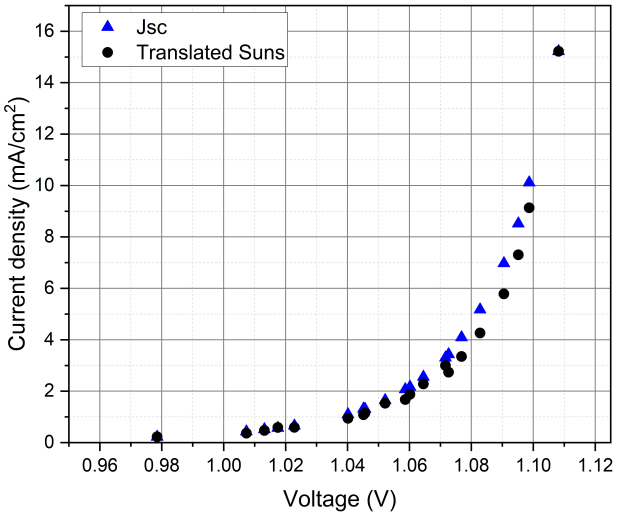

Figure 4.13: Effect of light intensity on Jsc of mini module

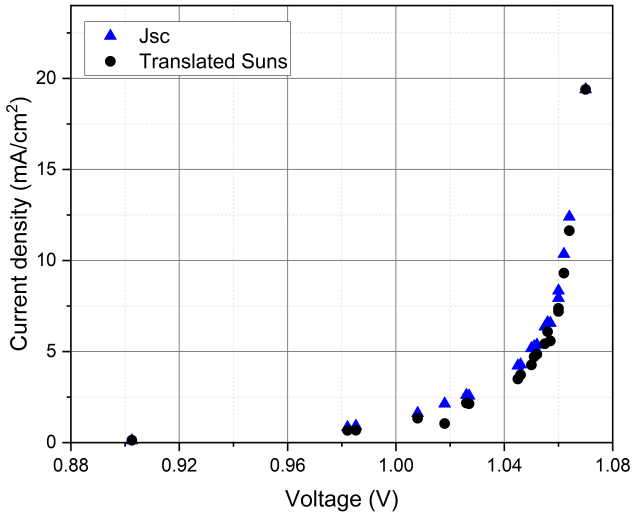

Figure 4.14: Effect of light intensity on Jsc of Pixel solar cells

As the light intensity is changed, all solar cell parameters will change including J_{sc}, V_{oc}, FF and efficiency. The dependence of light intensity (no.of suns) with respect to the short circuit current density is shown in the Figure 4.12, 4.13 and 4.14 for the two modules and a pixel cell respectively. This is compared in each case against the current-translated Suns constructed without the effect of series resistance. This, along with the results discussed in previous sub-section provides insight into the quality of the modules and cell used. For any sample, J_{sc} is desired to increase linear to light intensity. The same is viewed from the curves with slight deviation for mini module and pixel cell. Since J_{sc} at 1 Sun is taken as the translation point for Suns-Voc curve, the deviation is a measure of the actual extent of series resistance present in a sample at a given light intensity. The measurement of a higher Jsc relative to the translated Suns presents a possible overestimation of the effect of Rs on the samples, particularly at higher light intensities.

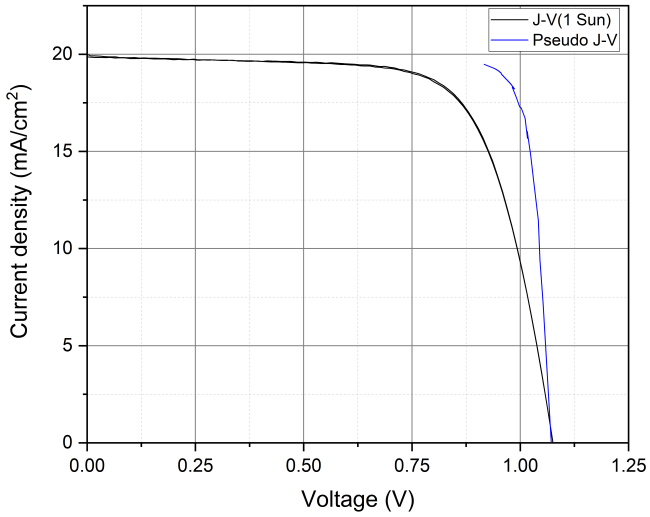

Figure 4.15: Pseudo J-V curve and J-V (1Sun) for perovskite large module

The result from testing superposition principle for large module was positive for a certain voltage level, which led to trying the exercise of constructing the pseudo J-V curve. The comparison of the pseudo J-V curve made by Suns-Voc method (or Jsc-Voc method) and the standard J-V measurement under one Sun is shown in Figure 4.15, 4.16 and 4.17 for large module, mini-module and pixel cell respectively.

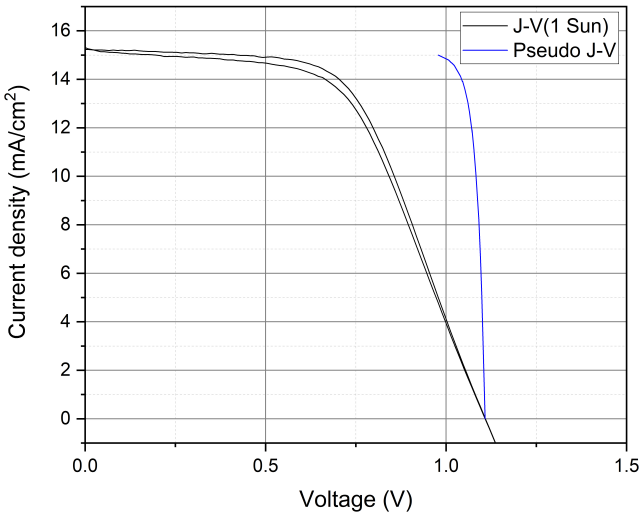

Figure 4.16: Pseudo J-V curve and J-V (1Sun) for perovskite mini module

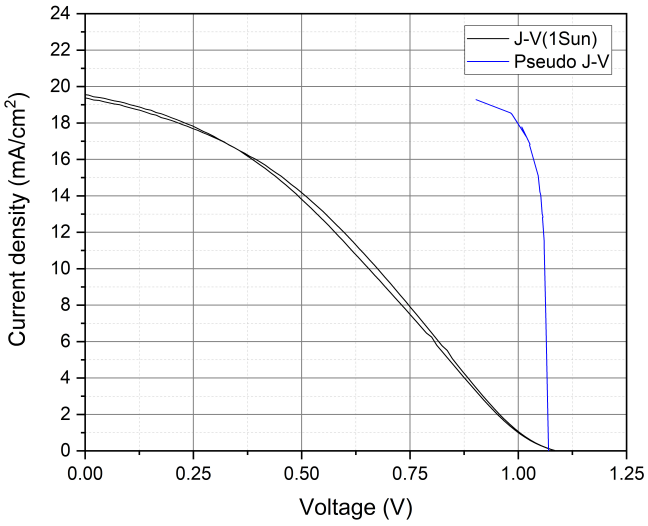

Figure 4.17: Pseudo J-V curve and J-V (1Sun) for perovskite solar cells

After plotting the pseudo J-V using Equation 3.2, the pseudo FF is calculated based on the graph. Table 4.4 shows the difference in FF obtained using Jsc-Voc(Suns-Voc) free from series resistance and FF calculated from standard J-V curve at one sun.

The Sun-Voc technique is used in this project to characterize the perovskite module and perovskite

Device	p-FF(%)	FF(1 Sun)
Large perovskite module	85.91	72.89
Perovskite mini module	88.4	57.75
Perovskite solar cell	87.80	35.5

Table 4.4: Pseudo FF from Jsc-Voc (Suns-Voc) and FF from J-V measurement

solar cells. The experiment is performed where the open circuit voltage is monitored during the variation of light intensity. Superposition principle should hold to be able to analyze a cell using the Suns-Voc method. A pseudo J-V curve as shown in the above Figures 4.15, 4.16 and 4.17 is built utilizing the recorded voltage, intensity, and Jsc of the module or cell based on this assumption. The theoretical maximum limit according to the SQ limit for a PSC is around 90% [66]. The p-FF(pseudo FF) computed using the pseudo J-V curve were 85.91%, 88.4% and 87.80% for large module, mini module and pixel cell respectively. Because there is no current flow during the measurement, this pseudo J-V curve is what the perovskite solar module or cell would have if there was no Rs. The comparison of Pseudo JV curve with the standard JV curve measured at one sun irradiance is used to determine Rs.

There are two types of series resistance i.e. Rs(light) which gives the series resistance under light and Rs(dark) that gives the series resistance under dark conditions. Suns-Voc method is used to calculate series resistance under illuminated conditions (Rs(light)) using light J-V curve which may get affected due to other factors. However, dark J-V curve can be used to calculate series resistance without illumination. Situations such as if PSCs have low charge collection and low diffusion, then it may result in overestimation and underestimation of Rs(series) and Rsh(shunt) respectively which will not happen if dark J-V curve is used to calculate Rs and Rsh. Under dark conditions, the dark J-V curve is fitted with 2 diode equation. Rs and Rsh can be extracted from the result at upper voltage part for Rs and lower voltage part for Rsh [61]. In order to reduce different components of Rs and also to decrease the bias dependency of photo-current, doping of ETL/HTL layer or doping of perovskite could be done which will increase the overall FF and thus improving the efficiency of PSC [66].

4.4. Conclusion

The aim of this section is to answer the first research question which were ”What are the constraints on applicability of superposition principle and Suns Voc on perovskite solar cells/module?”. Three different samples of perovskite were used to perform the experiment.

Light and dark J-V characteristics of the perovskite device were analysed and different external parameters were obtained. The power conversion efficiency calculated were around 14%, 9% and 7.5% for large perovskite module, mini perovskite module and perovskite solar cell respectively. Dark J-V curve shifted by Jsc is plotted to compare with light J-V i.e under one sun illumination which proves the invalidity of the Superposition principle. An alternate method is used again to test the validity of the superposition, where the device were exposed to different illumination level and J_{sc}-V_{oc} points obtained from each J-V curve were compared with the dark J-V to prove that the superposition principle does not hold for perovskites.

It was viewed that the existence of series resistance could be the major reason for failure of the principle. For large modules, the deviation is seen at higher voltage (according to method 2) which could be due to the influence of non radiative recombination. In case of pixel cells, the impact of Rs is larger which can originate from recombination at bulk or interfaces. The mini module shows a different trend than the large module and pixel cell where voltage is higher at lower intensities than the dark voltage and then increases with intensities. This deviation at higher intensity could be due to the bulk recombination. The behavior of mini module is further studied in the next chapter where it is exposed at different temperature and illumination level. Also, one of the possible reason of failure of the superposition principle could be the bias dependency of the photocurrent

which is supported by the literature.

The Suns-Voc method used to characterize the perovskite module/cell is implemented and pseudo J-V curve were constructed as an exercise. The pseudo FF calculated from this exercise were 85.91%, 88.4% and 87.80% for large module, mini module and pixel cell respectively. The theoretical maximum FF limit(SQ limit) of PSCs is around 90% for PSCs with Voc = 1.28V and Jsc = 27.3mA/cm^2 for a material of bandgap of 1.55 ev [66].

5

Effect Of Temperature On Performance of Top Perovskite Cell In Tandem Device

To have a detailed understanding of the perovskite module in outside environment, measurements must be taken in the lab at various temperatures and light intensity. This chapter aimed to answer the main research question by answering the second sub-question introduced in section 2.5 which were ”How does the perovskite module behave under the influence of different temperature and light intensity ?”. The chapter begins with the description of the electrical parameters and the relation between these parameters and temperature in section 5.1. Thereafter, the methodology used and the steps taken to perform the experiment is explained in section 5.2. Next in section 5.3, the results obtained from the experiment is evaluated and discussed in this part. Lastly, the chapter ends with the conclusion in section 5.4.

5.1. Temperature dependent electrical parameters

It is generally known that the performance of photovoltaic devices, and hence the maximum power production of solar cells, varies with temperature. As a result, when designing pv systems for actual outdoor applications, where changes in temperature take place throughout the day and year, it is critical to consider the temperature coefficients of the basic device J-V parameters such as open-circuit voltage (V_{oc}), short-circuit current (I_{sc}), fill factor (FF), and efficiency or maximum power point (P_{mpp}).

Open circuit voltage: The variable primarily impacted by a change in temperature in conventional solar cells is V_{oc}. The open circuit voltage of a solar cell is the voltage at which the overall rate of photogeneration equals the rate of recombination, resulting in no current flowing through the circuit. The temperature dependency of the generation-recombination balance is indicated by its relative change with temperature. The analysis of V_{oc} with T elucidates the major recombination processes.

The equation used to express V_{oc} for a traditional inorganic solar cell can be given as :

$$V_{oc} = \frac{nkT}{q} ln(\frac{Jsc}{Jo}) \tag{5.1}$$

where k is Boltzmann’s constant, n is ideality factor, Jsc is the short circuit current density and Jo is the diode saturation current density. For PSCs, it has been found in the literature that Voc decreases with increase in temperature, thus showing similar behavior as compared to other conventional solar cells.

Short circuit current: When the electrodes of a solar cell are short circuited, the current that passes through the external circuit is known as short circuit current. For a conventional solar cell, the short circuit current generally increases slightly with rise in temperature due to decrease in band gap energy. The change in short circuit current (I_{sc}) with temperature is smaller as compared to the change in Voc, however even small changes in bandgap energy can have an impact on I_{sc}. The temperature dependence of Jsc exhibits a linear trend for PSCs, although it is unclear how Isc varies with temperature. Overall, research shows that Isc decreases with increase in temperature over 25°C, but Isc may increase or decrease between 0°C and 25°C [21], [47].

Fill factor: The Fill Factor (FF) is a relationship between a cell's open circuit voltage and short circuit current and the maximum power that can be produced from it. It represents the lowest cost to get the photogenerated charges from the cell into the circuit, and it is related to the best current-voltage trade-off..This optimum is determined by the balance between generation and recombination, as well as the transport losses caused by current flow across the circuit at MPP. The FF of a solar cell is given by the below equation :

$$FF = \frac{Pmmp}{Isc \cdot Voc} \tag{5.2}$$

where Pmpp is the maximum power extracted of a solar cell.

Efficiency: The ratio between the maximum produced power and the incident power is used to determine a solar cell's efficiency. By fitting the efficiency dependency on temperature to a linear model, the absolute temperature coefficient of photovoltaic cell efficiency may be calculated. It can be calculated as follows :

$$\eta = \frac{P_{\text{max}}}{P_{\text{in}}} \tag{5.3}$$

where P_{in} is the incident power and is the product of irradiance with the area of the photovoltaic cell.

5.2. Experimental method

Solar cells in the field operates at different temperature with varying light intensity (depending on different climate conditions), which leads to changes in the performance of solar cell. Also long term operating stability is required for solar cell applications. This is particularly important for perovskites, which have the most positive unique properties compared to other high-efficiency solar cells. The most significant feature of PSCs is ion migration. One of the major common stability tests for assessing perovskite degradation in the lab is subjecting the device to varying light intensities and elevated temperatures.

A 4 cm^2 perovskite/Si tandem module(4T) was used to experimentally study the performance and the temperature dependence of the electrical parameters were investigated. Under simulated AM 1.5 G sun irradiation, the I-V parameters of the perovskite solar module were measured using a Keithley 2400 source meter. Using a Si reference cell, the light intensity was calibrated to 1000W/m2. The Figure 5.1 shows the tandem module used for the experiment. The top module is of perovskite with 6 sub-cells connected in series and the bottom module is of Silicon.

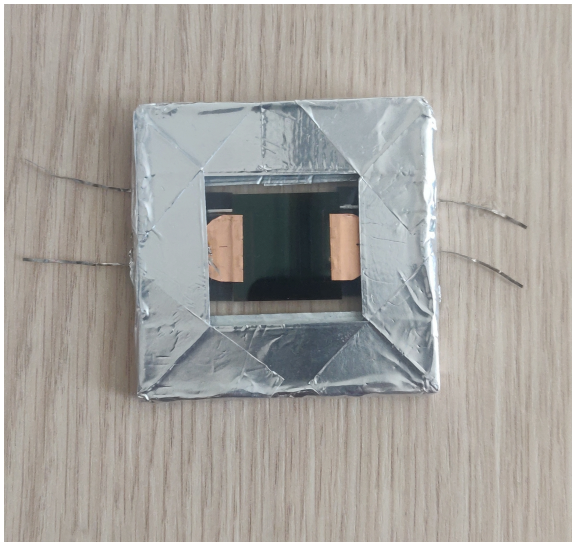

Figure 5.1: Perovskite/Si tandem module of size 4cm^2

J-V characteristics of the module were investigated at different light levels varying from 1000W/m^2 to 110W/m^2 using gray filters, with the temperature of the module ranging from 15°C to 55°C for each level of illumination. The temperature was increased by 10°C at each step and the module was stabilized by light soaking at MPP to lower the hysteresis at every level before the measurement series was performed. The tandem module used for the experiment has perovskite as a top layer and Si as a bottom layer. A thermostatic chuck is used to vary the temperature of the device. The top device (perovskite) is exposed to different illumination level at various temperature while the voltage of the bottom device (Silicon) is measured simultaneously using multimeter at different temperature and illumination levels. Using the temperature co-efficient of Si which is known, the bottom device is used as a temperature sensor to evaluate the calibrated temperature of perovskite from the observed temperature of a thermostatic chuck. The temperature coefficients of different electrical parameters are extracted from the experiment and are compared with the literature.

5.3. Results and Discussion

The impact of temperature on perovskite module is investigated by determining temperature coefficients of the J-V parameters. The silicon module in the tandem device are made of PERC solar cells which reduces rear recombination and allows more sunlight to be captured by adding a dielectric passivation layer on PERC. The temperature coefficient of silicon solar cell depends on recombination current density(J_0), which depends on silicon substrate and device passivation schemes. The voltage temperature coefficient of silicon solar cell (bottom layer in tandem device) is, $K_{th\text{-}V}$= -2mV/°C which was established from evaluation of substrate and passivation schemes. Figure 5.2 shows the relation between voltage and temperature of c-Si module(bottom layer of tandem) at 1 sun illumination when the temperature of the module is regulated using thermal chuck from 15°C to 55°C. As seen from the Figure 5.2, the voltage obtained is lower than the voltage for standard Si under AM 1.5 because Si module is on the rear side of the tandem device, thus only absorbing the transmitted light. Also preconditioning done to stabilize the perovskite module(top device) further reduces the voltage.

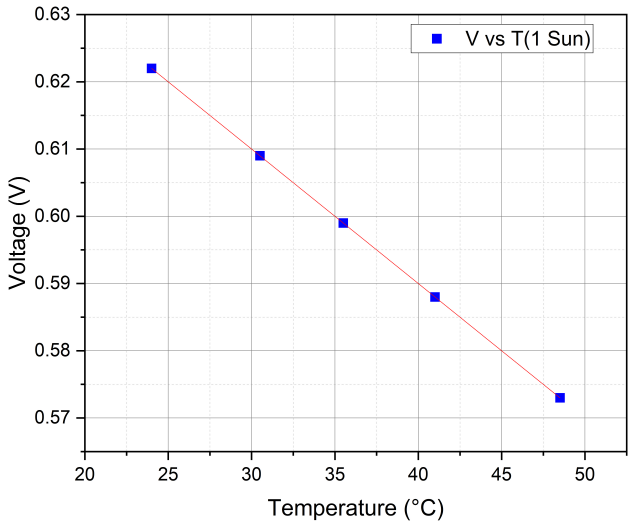

Figure 5.2: Voltage vs temperature (Si module - rear side of tandem device) under 1 sun illumination

Observed temperature(°C)	15	25	35	45	55
Calibrated temperature(°C)	24	30.5	35.5	41	48.5

Table 5.1: Observed and Calibrated temperature

The table 5.1 shown above gives the temperature obtained after calibrating using the voltage temperature co-efficient and the measured voltage of silicon module as explained before.

The behavior of the performance characteristics of perovskite mini module with regard to temperature was examined in order to explore the temperature-induced changes in top layer of tandem device (perovskite module) : Open circuit voltage(Voc), Short circuit current density(Jsc),Fill Factor(FF) and Power conversion efficiency (PCE).

The open circuit voltage (Voc) is given by the measurement of the electro-chemical potential of the photo-generated charge carriers. As shown in Figure 5.3(a),when the temperature of the perovskite mini module is increased from 15°C to 55°C (Observed temperature) a linear decrease in the open circuit voltage is observed at 1 sun. The voltage temperature co-efficient of the perovskite mini module (having 6 sub-cells) is $K_{th\text{-}Voc}$ = (-5.18 ± 1.67)mV.°C^{-1} and $K_{th\text{-}Voc}$ = (-0.86 ± 0.28)mV.°C^{-1} per cell. After normalizing at STC (i.e. 25°C and 1 Sun), the temperature coefficient of perovskite module is, $K_{th\text{-}Voc}$ = -0.079%.°C^{-1} (ignoring the uncertainty of the value). For PSC, several research has been done on temperature dependency in performance parameters. Recent report suggests that Voc drops with temperature having $k_{th\text{-}Voc}$ in the range from -0.074%.°C^{-1} [12] to -0.4%.°C^{-1}[5]. In 2020, Jost et al. [38] evaluated the performance of a PSC at outdoor and under lab with similar conditions. $k_{th\text{-}Voc}$ = -0.12%.°C^{-1} was obtained at laboratory conditions in the temperature range of 25°C to 85°C. The results (i.e. $k_{th\text{-}Voc}$) obtained in this study are within the range observed in literature.

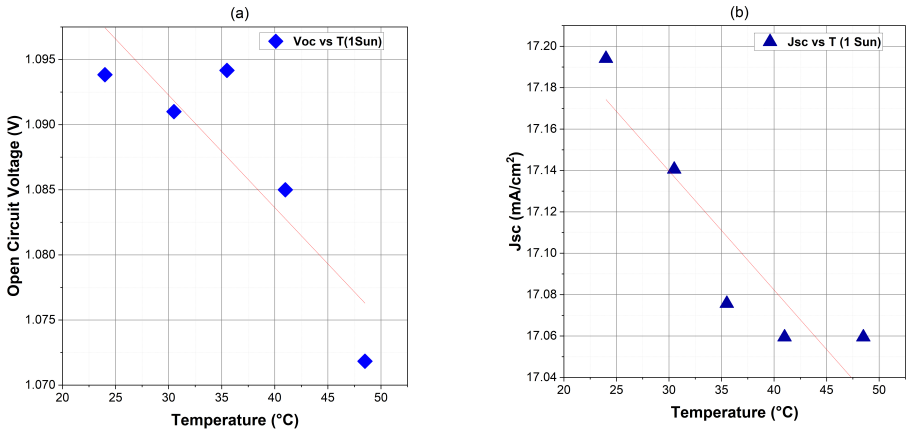

Figure 5.3: Temperature dependence of (a)Voc and (b)Jsc under one Sun illumination

The variation in the ratio of rate of photogenerated charge carriers and recombination rate in the solar cell are the main cause for the reduction in Voc. As temperature increases, the bandgap of PSC widens. This change is less sensitive to the changes in Voc with temperature because the relative voltage loss is less as compared to the voltage loss with temperature for the device with narrow bandgap [26]. Thus the change in rate of photogenerated charge carriers will not be large. When the temperature rises, the intrinsic carrier concentration rises, causing the dark saturation current to rise and hence decreases the Voc. When the temperature of the perovskite mini module was cooled from 55°C to 15°C , the open circuit voltage was measured again at 1 sun and a difference of 0.27% was observed from the initial measurement. Thus the short term degradation effect of the perovskite mini module due to the experiment can be ignored.

Jsc may be represented as a linear relationship with respect to temperature. In a solar cell, the Jsc is equal to the ideal current multiplied by the collection fraction. The ideal current is the current that might be produced if all incident photons with energies greater than the bandgap were converted without losses, where as collection fraction depends on various factors such as parasitic absorption, transmission, reflection and recombination in the solar cell.

In PSCs, the increase in temperature leads to widening of bandgap and thus causes a reduction in ideal current, whereas collection fraction generally increases with temperature [26]. Thus, the dominating factor may cause an increase or decrease of Jsc with temperature. It is observed from Figure 5.3(b) that the Jsc decreases with temperature very slightly. Under one sun, the Jsc drop for ΔT = 40°C is around 0.022 mA/cm2 and it yields a current temperature coefficient $k_{th\text{-}Jsc}$ = (-0.00575 ± 0.0015)mA/cm^2°C^{-1}. After normalizing with respect to 1 sun conditions, the current temperature coefficient is $k_{th\text{-}Jsc}$ is -0.033%°C^{-1}(neglecting uncertainty). Similar trend of Jsc with temperature is seen in literature with $k_{th\text{-}Jsc}$ of -0.054%°C^{-1} [38] and -0.9%°C^{-1} [5] for PSC.

Furthermore, the Voc is compared at different light intensities in the range mentioned above. Figure 5.4 is a semi-logarithmic plot between open circuit voltage and light intensity and the logarithmic dependence between them is apparent. It is observed that Voc increases with increase in light intensity. It shows that Voc increases as the generated charge carriers, i.e. the electron and hole concentration in the corresponding semiconductor increases, however the charge recombination rate may not be considerably enhanced at around one Sun condition.

The ideality factor was calculated for each of the temperatures using slope from each curve plotted above. The equation used to calculate ideality factor, n is given as :

$$n = \frac{slope}{kT.q^{-1}} \tag{5.4}$$

where k = Boltzmann constant, T = Temperature of the perovskite module and q = electron charge

The absolute ideality factor varies for different temperatures and very high value was obtained ranging from 5.68 to 6.12. This ideality could be due to heterogeneity of the surface of the mini module and also shows that the free carrier recombination dominates the perovskite mini module.

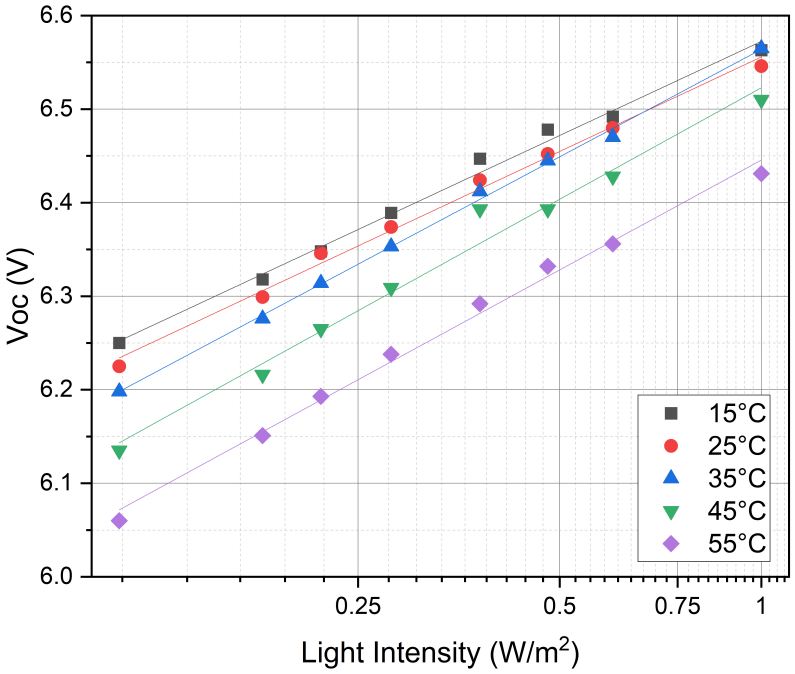

Figure 5.4: Voc dependence on light intensity and temperature of perovskite mini module

Fill factor of the solar cell relates the open circuit voltage, maximum power produced and the short circuit current density. The impact of temperature on the fill factor of the perovskite module is investigated in this part. As it be can seen from the Figure 5.5(a), FF shows a linear increase with temperature although the open circuit voltage (Voc) has shown a decrease with increase in temperature. An increase of approximately 8% is observed over ΔT = 40°C and a change of around +6.4% of FF of the device from 25°C to 55°C is measured. For other standard solar cells such as c-Si, GaAs, CdS and CdTe, a decease in fill factor is observed with increase in temperature [59].

This behavior could be possible due to decrease in Rs at higher temperature which may result in decreasing the barrier and hence will improve the charge carrier extraction at elevated temperature. The investigation of dark current with temperature will provide the temperature dependence of Rs. If Rs is not responsible for this trend of FF, then it could be said that the increase is due to the trap states and defects in the perovskite layer. As temperature rises, lesser charge carriers are trapped and the electric field will become more uniform due to the existence of carrier trapping by defect states. As a result, the net impact of temperature is a decrease in recombination and a rise in FF.

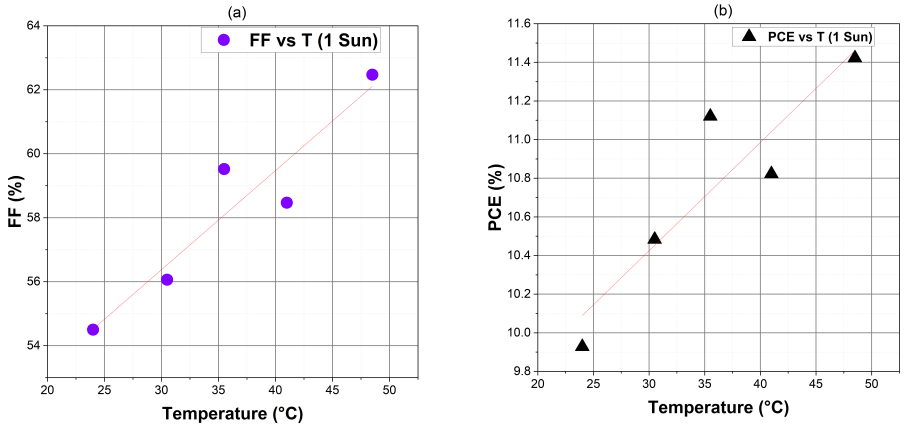

Figure 5.5: Variation of (a) FF and (b) PCE with respect to temperature at 1 Sun illumination

The Figure 5.6 shows the J-V curve under one sun irradiance having both the forward and backward scan results at 25°C and 55°C. At room temperature i.e. 25°C, hysteresis of around 4.2% was observed. At higher temperature, a decrease in hysteresis was viewed i.e. around 2% at 55°C. This S-Shape kink appearing in the J-V curve at low temperature indicates the deterioration of the charge carrier extraction and hence lower FF at low level temperature as compared to elevated temperature conditions (Figure 5.7).

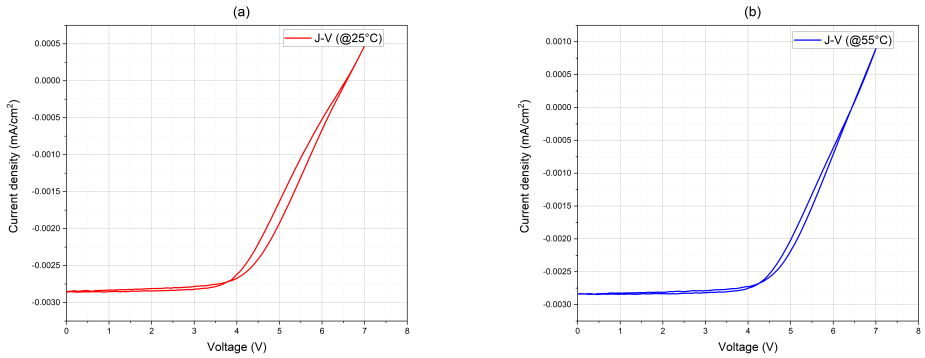

Figure 5.6: Light J-V curve at (a)25°C and at (b)55°C

The light intensity is varied from 100% to 11% of one sun with increase in temperature and the variation of light intensity with FF is depicted in Figure 5.7. It shows that at lower light intensities, FF is higher, indicating that smaller area devices may suffer losses due to series resistance in the contacts. FF depends on Voc and on resistance losses, thus a higher Voc can potentially improve the FF. But at higher intensity level, the resistance losses are the dominating factor which results in decrease of FF.

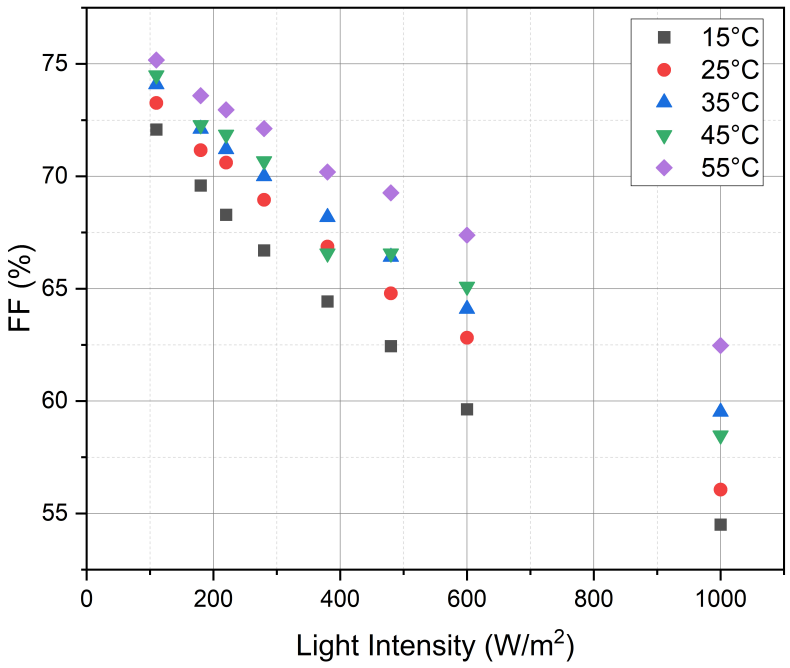

Figure 5.7: FF vs Light intensity at each temperature level

After following the dependency of temperature on FF, the changes in PCE with temperature is also observed as shown in Figure 5.5(b).As noticed above i.e. the increase in FF with temperature, similar behaviour was obtained for PCE. The PCE increases linearly with increase in temperature. As shown in Figure 5.5(b), PCE of around 10% was observed initially. Upon the temperature change to 35°C, the PCE rises to around 11% and it shows the similar increasing trend at further higher temperature. An increase of total 1.5% was obtained for temperature change of 40°C. After lowering the temperature back to the initial value, PCE of around 10.5% was calculated having a difference of 0.5% from the initial condition. The linear dependence of PCE vs T was viewed with a slope of (0.055 ± 0.014)%°C^{-1}.The temperature coefficient obtained is then normalized at STC to get $k_{th\text{-}PCE}$ = 0.56%.°C^{-1} (neglecting uncertainty). According to the literature, negative $k_{th\text{-}PCE}$ is seen more often which means decrease in PCE with increase in temperature. Fu et al. [13] measured $k_{th\text{-}PCE}$ of -0.18%°C^{-1} for a very small PSC. In 2020, Subhranshu and others [5] evaluated the temperature co-efficient of -2.1%°C^{-1} of carbon based PSCs. The result obtained in this study is not common to PSCs.

This behavior could be attributed with respect to the FF. A rise in temperature causes an increase in FF, which could be caused by a decrease in charge carrier diffusion resistance, and it also facilitates efficient charge extraction of photo-generated charge carriers. This rise in FF compensates for the expected drop in Voc at high temperatures. As a result, PCE rises with temperature.

5.4. Conclusion

This chapter discussed the behavior and performance of a perovskite mini module when temperature and illumination is varied. It was aimed to answer the third research question which was "How does the perovskite module behave under the influence of different temperature and light intensity ?". The temperature of the tandem module was increased from 15°C to 55°C (observed temperature of thermostatic chuck) and the known voltage temperature co-efficient of Si device was used to calibrate and obtain the real temperature of the perovskite mini module. The J-V analysis of the module was done for different illumination intensity varying from 100% to 11% of one irradiance at each temperature level.

The temperature dependency of V_{oc} was characterized. As temperature increases, a linear decrease in Voc was observed and a voltage temperature coefficient i.e. $K_{th\text{-}Voc}$ = (-5.18 ± 1.67)mV.°C^{-1} (for module) and $K_{th\text{-}Voc}$ = (-0.86 ± 0.28)mV.°C^{-1} per cell was calculated. The decrease is due to the rise of dark saturation current because of the increase of intrinsic carrier concentration. Also, the logarithmic relation between voltage and illumination intensity helps to determine the ideality factor of the device.

The short circuit current density of the perovskite module decreases slightly with increase in temperature and the current temperature coefficient of (-0.00575 ± 0.0015)mA/cm^2.°C^{-1}. Additionally, the variation of FF with temperature was observed. The FF was found out to be increasing with temperature even though both V_{oc} and J_{sc} decreases with temperature. The variation of FF with light intensity was observed which showed drop in FF at higher irradiance. This could be because of increase in recombination at stronger light intensity. At high temperature, the higher value of FF could be due to enhanced charge carrier extraction with lower Rs. This results in increase in PCE with rise in temperature. Thus, it can be said that the temperature dependency of charge extraction could be the underlying reason for the temperature dependence of the performance of perovskite module. The impact of temperature on Voc and Jsc for perovskite corresponds to the values obtained in literature.

6

Towards MPP Tracking Of Perovskite Solar Module

The maximum power point fluctuates with temperature and irradiance in outside field conditions, affecting the performance of a solar module. Thus, the MPPT algorithm is significant in PV systems since it maximizes power output under given conditions, thereby increasing efficiency. The aim of the chapter is to answer the final sub-question of the study which was " How to track the true MPP of the perovskite solar cells/module in laboratory ? ". The beginning of the chapter is with the background of the performance measurement techniques for the PV technologies in section 6.1. Then in section 6.2 brief description of some of the most common algorithms or methods used to track MPP . The next part i.e. in section 6.3, explanation of the protocol used to measure the maximum power of perovskite modules in the laboratory conditions is discussed. Thereafter, the protocol is validated by showing results in section 6.4 and later in section 6.5, the chapter is concluded.

6.1. Background

The amount of electricity generated by a PV module is determined by the operating temperature, the amount of solar irradiation falling over the array of the PV cells, and the load attached. The non-linear relationship of the J-V characteristics determines the power output of the photovoltaic cells. Various factors can impact the power output such as variation of the solar intensity, the temperature through out the whole day, shading due to dust, clouds. These factors will change the maximum power point. Also, because of the non-linear connection between current density(J) and voltage(V) of the photovoltaic module, each weather condition has a unique MPP (maximum power point) which changes with irradiance and temperature of the atmosphere.

The J-V curve is used by the researchers to quantify the performance of PV at STC which expresses power as a function of voltage difference across the device electrodes. Usually, the J–V curve is determined by changing the voltage across the device and measuring the current at each voltage. J–V curves are achieved in a step wise manner, with each voltage held for a certain amount of time (the dwell time) before measuring the current and suddenly moving to the next voltage. The current density of good commercial Si solar cells (especially p-type) stabilizes rapidly (less than a millisecond) to a value based on the present measurement circumstances rather than the device's previous history. Thus, the entire J-V curve can be obtained with short dwell time within milliseconds to seconds.

However, for other PV technologies, the situation is more complicated, necessitating the development of modified measuring techniques. As an example, DSSCs (dye-sensitized solar cells - belong to the thin film solar cell category), that take longer response times to changes in bias, may need

J–V sweep duration of 5s or more to provide sufficient current stabilization at each bias level [4]. Other thin film PV technologies like CIGS, CdTe and a:Si can be evaluated with rapid J-V scans although they demand careful stabilization procedure(i.e. preconditioning) prior to measurements [42]. Preconditioning gives consistent performance measurements for CIGS, according to Kenny et al., but CdTe modules require at least five cycles to properly stabilize, and even nine cycles were inadequate to achieve stability in a:Si/m:Si modules [42].

Perovskite Solar cells are facing challenges that are greater than other PV technologies. Hysteresis is the most well-known problem, and it refers to the variations in J-V sweeps which is based on speed of J-V scan, scan directions (forward and reverse), step size, dwell duration, initial bias, and the intensity of light on the device. Thus, the PCE (or P_{max}) from J-V measurements may not be reliable and accurate because of the hysteresis behavior of PSC. Some PCEs obtained from J-V measurements published in the literature may have greatly overstated performance. For evaluating PCE, P_{max} at steady-state must be determined, and many methods other than the standard J-V curve measurement described in IEC 60904-1 are applied as already discussed in section 2.4 of Chapter 2. These approaches may be divided into three categories : (1) MPPT (Maximum power point tracking), (2) Steady state power output, and (3) Dynamic J-V measurements.

Below section describes the most commonly used MPPT techniques nowadays to track P_{max} and to evaluate PCE.

6.2. Standard MPPT method

To obtain the maximum PCE under different conditions and loads, an algorithm of MPPT (maximum power point tracking) is often employed. MPPT is used in the lab when the J-V curve cannot be obtained reproducibly for reasons beyond the control of the operator.

Different MPPT algorithms have been used previously such as Open circuit voltage method, Short circuit voltage method, P&O method (Perturb and Observe), Incremental conductance method. All of the MPPT methods discussed in this section are based on determining and adjusting the voltage until V_{MPP} is obtained.

(1) Open circuit voltage method : According to this method, the V_{MPP} is given by the product of V_{oc} with a constant K.

$$V_{\text{MPP}} = V_{\text{oc}} \times K \tag{6.1}$$

where K is depends on the type of solar cells. Changes in the V_{oc} can be measured easily, therefore changes in the V_{MPP} can be calculated simply by multiplying by K. Using above equation, this measurement is performed periodically to get Pmax (maximum power).

Despite the apparent simplicity of this technique, selecting an appropriate constant K value is challenging. For multi-crystalline PV modules, the value of K ranges from 0.73 to 0.80 [71]. Also, using a constant factor K provides for just an approximate approximation of the MPP. As a result, the operational point is generally not on the MPP itself, but rather close to it.

(2) Perturb and Observe (P&O) method: P&O method is also known as Hill Climbing method, as in this approach the PV module's operational point advances in the direction of increased power. The algorithm is sometimes referred to as a basic P&O algorithm since it is simple and easy to execute.

In this method, the operational bias of the PV cell is perturbed by a small increase or decrease. This results in the change in current density (ΔJ) and thus the change in power(ΔP) is extracted. If the change in power(ΔP) is positive, it is considered that the bias perturbation was successful in bringing the power output closer to the maximum power point, and thus more bias perturbations are applied in the same direction as before. But, if it is negative, it is established that the bias

perturbation shifted the output power away from the maximum power point and subsequent bias perturbations are applied in the opposite direction in order to bring the output power closer to the MPP.

As previously stated, the advantages of this method are its simplicity and convenience of implementation. However, there are some problems with the P&O algorithm that must be addressed. The operational point of this algorithm is never stable at the MPP, rather fluctuates around the MPP. However, by using very small perturbation steps around the MPP, this meander can be reduced. In addition, this algorithm has problems interacting with rapidly changing irradiance [43]. As a result, the algorithm's speed of convergence slows down, which is one of the key figures of merit for MPPT methods. Thus, extreme variations in weather have a significant impact on the effectiveness of the algorithm. Also, it is difficult to extract maximum power using this method during partial shading that results in local maximum in P-V characteristics.

(3) Incremental Conductance Method: Hussein et al. [43] introduced the "Incremental Conductance" method as an alternative to the "P&O" method. To eliminate the drawback of the P&O algorithm of fluctuating the operating point around MPP, instantaneous conductance (I/V) is compared with the incremental conductance (dI/dV) in this method.

The voltage of MPP is monitored to ensure that (Figure 6.1) :

$$\frac{dP}{dV} = 0 \tag{6.2}$$

As power of the PV module can be given as; P = IV, thus the equation can be written as

$$\frac{dP}{dV} = \frac{d(IV)}{dV} = I + V\frac{dI}{dV} \tag{6.3}$$

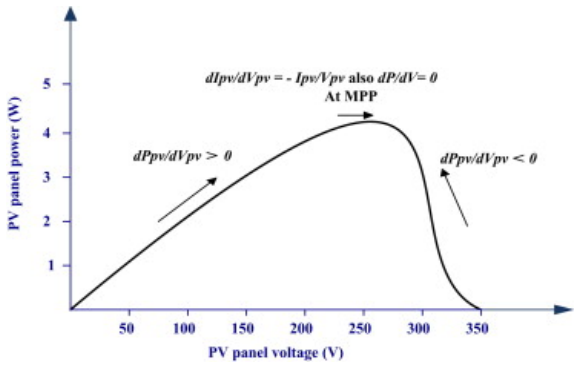

Figure 6.1: Characteristic curve of PV module showing variation of dP/dV [43]

Also, dI/dV can be approximated as ΔI/ΔV, if the sample steps are small. Therefore, using equation 6.2 and equation 6.3, the derivative may be used to analyze if the PV system is performing at its MPP or not.

$$\frac{dP}{dV} = 0; \frac{\Delta I}{\Delta V} = -\frac{I}{V} \qquad for \qquad V = V_{\text{MPP}} \tag{6.4}$$

$$\frac{dP}{dV} > 0; \frac{\Delta I}{\Delta V} > -\frac{I}{V} \qquad for \qquad V < V_{\text{MPP}} \tag{6.5}$$

$$\frac{dP}{dV} < 0; \frac{\Delta I}{\Delta V} < -\frac{I}{V} \qquad for \qquad V > V_{\text{MPP}} \tag{6.6}$$

The Incremental conductance method, as illustrated in the P-V curve in Figure 6.1 at MPP, is based on equation 6.4. Using equation 6.5 and 6.6, it can be viewed that the operating point is on the right and left side of the P-V curve respectively.

Under steady state conditions, the ”Increamental conductance method” oscillates less around the MPP than P&O method, thus making this method more efficient. Additionally, because of the short sample intervals, it is less sensitive to changing illumination conditions. However, in highly variable circumstances and partial shading, this approach may become less effective. Also, the hardware implementation of this method is very complex which is the major drawback of this method.

For PSCs, a P&O method have been proposed that dynamically changes the step size of voltage and sampling time when the dynamic response of the device varies. A study done by Cimaroli et al. proposed a predictive MPPT method (modified PO method) that calculates steady state power when the response of current is fitted with voltage perturbation having a bi-exponential function [15]. When devices show J-V hysteresis, even PO and predictive MPPT methods may become trapped in local performance maxima [57]. These method also shows oscillations of the power and voltage [67].

The three methods to determine MPP as mentioned in section 6.1 differs in the way voltage is adjusted. In MPPT and dynamic J-V measurement, voltage is adjusted automatically with the help of computer program while steady state approach requires manual adjustment of voltage.

Here in this study, a new measurement protocol have been proposed that can be implemented in lab to track MPP and calculate P_{max} (or PCE). A large perovskite module (size 100cm^2) is used to track MPP using the proposed measurement protocol as discussed in the next section. The most important reason for executing this method is lack of the availability of software required to perform MPP test under laboratory conditions.

6.3. Measurement Protocol to track MPP

A useful flowchart for MPPT measurement is shown in Figure 6.2. This chart gives the user to conduct an experiment with the aim of accurately tracking maximum power output of perovskite solar cells/module in the laboratory conditions.

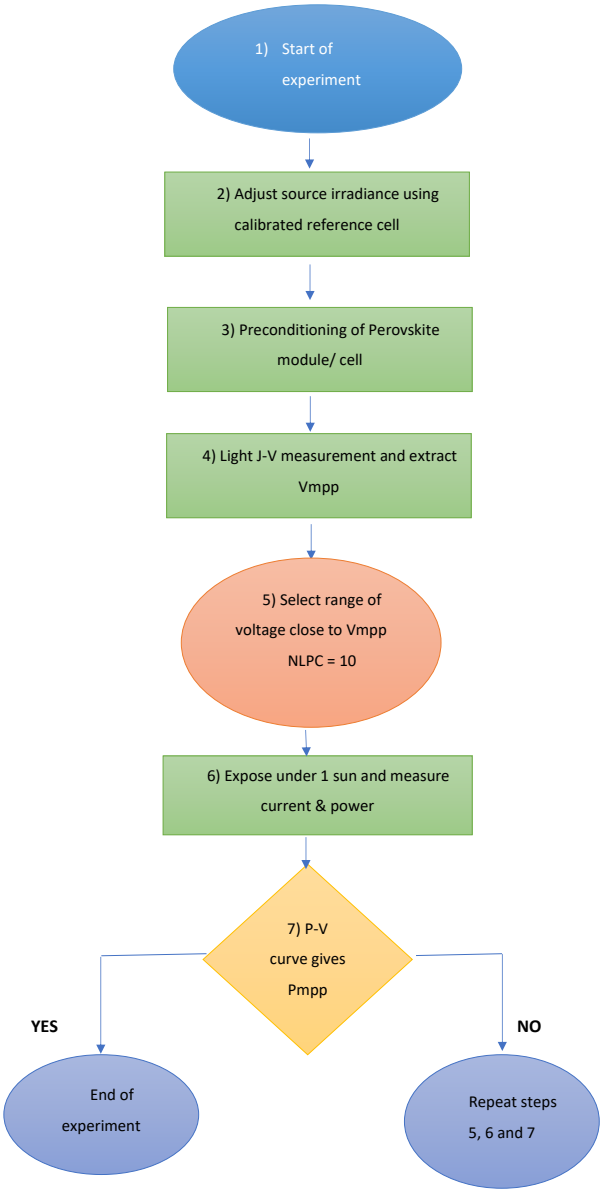

Figure 6.2: Flowchart for tracking MPP of Perovskite in lab

The experiment starts with adjusting the source irradiance of the solar simulator (WACOM) carefully with the help of calibrated Si solar cell. For perovskite solar cells/module, preconditioning is an important step required to stabilize the device and decrease the hysteresis. After pre-conditioning, the device is exposed under 1 sun and J-V measurement is done. The external parameters are calculated from the light J-V curve. Vmpp is also extracted from the curve which helps to select a range of voltage close to the maximum power point. The device is exposed again under one

sun irradiance for that particular range of voltage and the current is determined and hence gives the power output. P-V-T (Power-voltage-time) curve is generated and the analyses of the curve results in obtaining Pmpp(maximum power output).

If the generated curve does not provide the Pmpp, the experiment is repeated again by adjusting the range of voltage and increasing the number of time to repeat the pulse train of voltage. This step is repeated until the Pmpp is obtained for the device. After extracting the true Pmpp, efficiency of the device is calculated and compared with the efficiency obtained from the single J-V characteristics at STC.

6.4. Result

In this part, the protocol for the measurement of true maximum output power mentioned in the previous section has been applied for the perovskite module with a size of 100cm2. The same perovskite large module (with good FF) is used for the experiment which has already been discussed in chapter 2.

The experiment is performed in lab and is done to track the MPP which can be different from the MPP obtained from J-V characteristics. The maximum power output extracted from the J-V curve can be overestimated/underestimated. Thus, a new measurement method is followed and the approach is explained in the form of flowchart in previous section. Figure 6.3 is a representation plot of voltage and power as function of time.

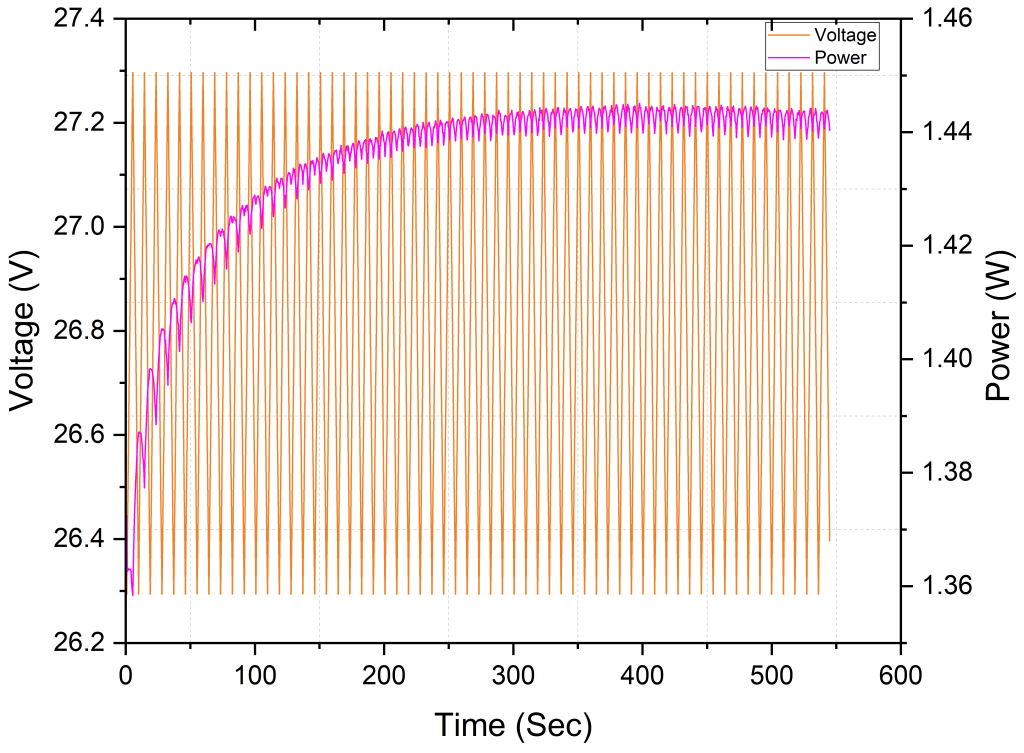

Figure 6.3: Graph of Voltage and Power with time to track MPP

After performing the J-V test under 1 sun in both direction i.e. forward and backward, Vmpp has been extracted. From the figure it can be seen that the voltage has been varied from 26.3V to

27.3V where the Vmpp (calculated from Light J-V) is 26.6V and 26.48V for forward and backward scan respectively. The current density is monitored and the power output is calculated from the result. It has been observed that the experiment takes approximately 9 minutes to attain a steady state, otherwise if enough time is not given for the measurement, there is a possibility to have unstable current which may underestimate or overestimate the maximum output power.

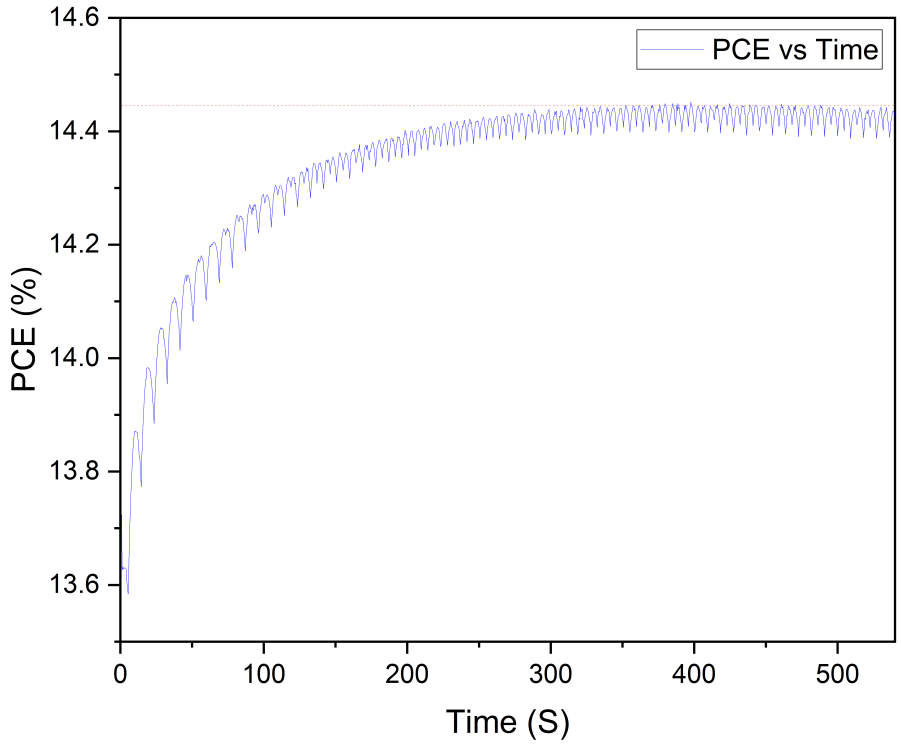

Figure 6.4: Power conversion efficiency vs Time

Figure 6.4 shows a maximum power point tracking profile for a large perovskite module(active area 92.5 cm^2) where PCE is plotted as a function of time. It can be viewed from the figure that the experiment takes more than 300 seconds to reach a steady state and maximum power output can be obtained. Using the MPP tracking profile, the efficiency of the perovskite module was determined to be 14.4% with the current density at MPP declining from 19.53mA/cm^2 to 17.98mA/cm^2 as compared from the values obtained through standard J-V characteristics. Table 6.1 shows the J-V parameters of perovskite module under STC.

Direction	Jsc(mA/cm^2)	Voc(V)	FF(%)	Efficiency(%)
Forward	19.76	1.07	73.17	14.39
Reverse	19.65	1.07	74.23	14.51

Table 6.1: JV parameters of perovskite module

Reliability of result : For accuracy of the result, generally P_{max} calculated using the MPPT method is compared with the value obtained from the dynamic J-V measurements [67]. The dynamic J-V method is a steady state method that can be employed when the conventional method

for measuring the J-V curve described in IEC 60904-1 is difficult to use [86]. In this case, P_{max} from standard J-V measurement is taken to compare as it has been discussed in the previous section (section 3.1) that the J-V curve obtained for large perovskite module has shown stability over a period of time.

Module	P_{max} by MPPT	P_{max} by J-V curve
Perovskite module	1.445W	1.440W

Table 6.2: P_{max} by MPPT and by standard J-V

In Table 6.2 a comparison of P_{max} is shown, where P_{max} of MPPT is obtained by using the algorithm and P_{max} determined by standard J-V measurement is the average of P_{max} obtained in forward and reverse direction. The difference between P_{max} values produced by the MPPT technique and the traditional J-V approach was 0.35%, as shown in Table 6.2, suggesting that the MPPT method established in this work is as accurate as a standard J-V measurement.

The measurement was conducted for the best performing perovskite module (FF = 73%). In this approach, the voltage estimated is close to the MPP obtained from J-V measurements which is a challenge to determine since different J-V curves will provide different MPP voltage. Also, it is not necessary that the chosen voltage from J-V curve will always be close to the true V_{mpp}. To determine PCE using this approach, steady state should be maintained at least for the duration of the measurement time. In addition, measuring the complete J-V curve in the range from SC (short circuit) to OC(open circuit) voltages is challenging since PCE can change over time for most PSCs. Moreover, because full steady-state is difficult to achieve, this approach may not be sufficient to avoid oscillation for PSCs with significant hysteresis. Thus, after looking into the limitations, it could be better to use MPPT algorithms if the software is available to conduct MPP test which should be free from oscillations to give accurate results.

6.5. Conclusion

In summary, a protocol has been applied for the tracking the true MPP for perovskite devices under laboratory conditions and provide maximum PCE. The result obtained will give the accurate MPP so that the Rs can be calculated at this point and different degradation test can be conducted at MPP to compare with outdoor conditions. In this study, the calculation of Rs has not been done as initially it was aimed to calculate using Suns-Voc method. The method has been tested by applying on the perovskite large module under STC and the result has been presented above. It was concluded that to track the true MPP, the experiment should be continued for more than 300 seconds. To achieve steady state, the test was conducted for approximately 9 minutes. For more accurate results, the perovskite module should be tested for a longer duration of time after achieving steady state. P_{max} values obtained from this approach were found to be reliable by comparing the values from the standard J-V measurement. The suggested approach can be implemented at varied temperatures and irradiance levels to replicate the results in outside conditions.

7

Conclusions and Recommendations

This chapter describes key findings from this master's thesis project and suggestions for further studies. Three different perovskites samples were used for the study which were fabricated by TNO Eindhoven partner in Solliance. The major goal of this project is to understand the behavior of perovskite solar cells as a top cell in tandem devices. It was done by the following key research question:

"How does the top perovskite solar cell in tandem device behave under real operating conditions ?"

Based on the main research question, three research sub-questions were derived. These sub-questions will be explored and answered in the next section.

7.1. Conclusions

7.1.1. Suns-Voc

This section answers the first research sub-question that were presented in section 2.5. The first question was "What are the constraints on applicability of superposition principle and Suns-Voc method in perovskite solar cell/module as a top cell in tandems ?". In order to answer this question two perovskite module (size of 100cm^2 and 4cm^2) and a PSC (18mm^2) were used to perform the experiment.The complete explanation of the result obtained was provided in Chapter 4. The results obtained from characterization of PSC using Suns-Voc method can provide important information about the power loss mechanism which is essential to understand the performance of perovskite during the real operating conditions.

For the analysis of Suns-Voc method, the principle of superposition should hold. Thus, the validity of superposition principle was tested using two different methods for perovskite module and solar cell. The result shows that the principle fails for perovskite devices. The presence of series resistance was thought to be a key factor for the failure of superposition principle. The result from testing superposition principle for large module (best performing module with FF of 74%) was positive for a certain voltage level and deviation (Jsc-Voc from dark J-V curve) was observed at higher voltage which may be due to the non-radiative recombination. In case of pixel cell, huge deviation was seen and the impact of Rs was observed larger which can originate from recombination at bulk or interfaces. Mini module showed different trend than both large module and pixel cell where voltage was observed higher at lower intensities than the dark voltage and then the voltage increases with intensities. Also, the invalidity of the superposition principle could be due to bias dependency of the photocurrent. Doping of ETL/HTL and perovskite layer could reduce the different components in Rs and also the bias dependency which will further improve the performance of PSC.

7.1.2. Temperature measurements

This section is referred to the second research sub-question stated as "How does the perovskite module behave under the influence of different temperature and light intensity ?" and it was answered in Chapter 5. Perovskite mini module (6 sub-cells connected in series with an active area of 3.7cm^2) was used to conduct the experiment. The results obtained from the experiment will provide a thorough knowledge of perovskite module operating under real world conditions and the result will also be useful to compute the energy yield of the module in real world operating situations.

The temperature dependency of different J-V parameters were characterized and temperature coefficients were calculated. It was observed that Voc decreases with increase in temperature and a voltage temperature coefficient of -0.079%.°C^{-1} was computed. This decreasing trend is due to the rise of dark saturation current because of the increase of intrinsic carrier concentration which increases with increase in temperature. Jsc of a perovskite module decreases with rise in temperature. The current temperature coefficient of a module was -0.033%.°C^{-1}. Also the variation of illumination intensity with Voc was plotted which helped to calculate ideality factor at different temperatures. High ideality factor was obtained from the result ranging from 5.68 to 6.12. This could be due to heterogeneity of the surface of the mini module and also indicates that the free carrier recombination dominates the perovskite mini module.

Furthermore, the change of FF with temperature was found. The FF was shown to increase with temperature, despite the fact that both Voc and Jsc decrease with temperature. The increased value of FF at high temperatures might be attributed to improved charge carrier extraction with lower Rs. As a result, as the temperature rises, the PCE rises as well and a temperature coefficient of 0.56%.°C^{-1} was calculated.

7.1.3. MPP measurement

Chapter 6 provided the explanation that was aimed to answer the third research sub-question which was "How to track the true MPP of the perovskite solar cells/module in laboratory ?". To answer this question, large perovskite module (31 sub-cells series interconnected with an active area of 92.5cm^2) was taken to perform the experiments.

At outdoor locations, the temperature and irradiation changes which led to change in maximum power point. This impact the performance of a solar module. Therefore, it becomes important to track the maximum power output under different environment conditions which can be done using MPPT algorithm. In this study, an alternative method was implemented to track the MPP using a new measurement protocol which was explained in section 6.3 of Chapter 6. The method used can be applied at different temperature and irradiance levels to produce results similar to outdoor conditions.

The proposed protocol was used to track the true MPP of a large module under STC. It was determined that the experiment needs be extended for more than 300 seconds in order to track the true MPP. The test lasted roughly 9 minutes to attain steady state. Pmax and PCE was calculated after achieving steady state and the result was compared with values obtained from standard J-V measurement to have reliability of result.

7.2. Recommendations

As discussed in Chapter 4, the superposition principle does not hold for PSCs and modules. It was concluded that the bias dependency of photocurrent could be one of the reasons for the failure of principle. In order to reduce the bias dependency, doping of ETL/HTL and perovskite layer can be performed. To execute this, simulation could also be done by increasing the doping concentration of ETL/HTL and perovskite layer. Simulation requires data of electrical and optical properties which could be obtained by measurement of perovskite devices. Pseudo J-V curve was constructed as

an exercise using Jsc-Voc technique. This method could also be validated by performing the J-V measurement of heterojunction c-Si solar cells with different gray filters and comparing the results obtained from Sinton Suns-Voc tool.

It is also recommended that the temperature dependency measurements of J-V parameters to be performed with multi samples of perovskite module and PSCs as well. Also this measurement can be repeated for several days to understand the stability and degradation of PSCs. Additionally, using the data obtained from the experiment, calculation of the overall energy yield could be done.

The MPP tracking done in this study using the proposed algorithm should be explored for several devices (perovskite module and PSCs) having high hysteresis. Further, this experiment could also be done at various temperature and irradiation level to have a better understanding of PSCs in real world conditions.

Bibliography

[1] Y. Shirai T. Miyasaka A. Kojima, K. Teshima. Organometal halide perovskites as visible-light sensitizers for photovoltaic cells. 2009. URL https://pubs.acs.org/doi/10.1021/ja809598r.

[2] K.K. Chin A.E. Delahoy, Z. Cheng. Carrier collection in thin-film cdte solar cells: Theory and experiment. *27th European Photovoltaic Solar Energy Conference and Exhibition*, pages 2837–2842, 2012. URL https://www.researchgate.net/profile/Alan-Delahoy/publication/295547168_CARRIER_COLLECTION_IN_THIN-FILM_CDTE_SOLAR_CELLS_THEORY_AND_EXPERIMENT/links/56cb1dfe08aee3cee54159ba/CARRIER-COLLECTION-IN-THIN-FILM-CDTE-SOLAR-CELLS-THEORY-AND-EXPERIMENT.pdf.

[3] Tom Aernouts. Tandem technology for solar cells: Boosting the efficiency to accelerate photovoltaic integration. *Energy Ville*, 2021. URL https://www.energyville.be/en/press/expert-talk-tandem-technology-solar-cells-boosting-efficiency-accelerate-photovol

[4] Giorgio Bardizza, Diego Pavanello, Roberto Galleano, Tony Sample, and Harald Müllejans. Calibration procedure for solar cells exhibiting slow response and application to a dye-sensitized photovoltaic device. *Solar Energy Materials and Solar Cells*, 160:418–424, 02 2017. doi: 10.1016/j.solmat.2016.11.012.

[5] Shubhranshu Bhandari, Anurag Roy, Aritra Ghosh, and Tapas Mallick. Perceiving the temperature coefficient of carbon-based perovskite solar cells. *Sustainable Energy Fuels*, 10 2020. doi: 10.1039/D0SE00782J.

[6] S. Bowden, V. Yelundur, and Ashish Rohatgi. Implied-voc and suns-voc measurements in multicrystalline cells. pages 371 – 374, 06 2002. doi: 10.1109/PVSC.2002.1190536.

[7] Levy M.Y. Bremner, S.P. and C.B Honsberg. Analysis of tandem solar cell efficiencies under am1.5g spectrum using a rapid flux calculation method. 2008. URL https://onlinelibrary.wiley.com/doi/abs/10.1002/pip.799.

[8] Egger D. Kronik L. Hodes G. Cahen D Brenner, T. M. Hybrid organic–inorganic perovskites: low-cost semiconductors with intriguing charge transport properties. 2016. URL https://doi.org/10.1038/natrevmats.2015.7.

[9] B.J. Bruijnaers. *Lead halide perovskite solar cells*. PhD thesis, June 2018. URL https://pure.tue.nl/ws/files/98002069/20180628_Bruijnaers.pdf. Proefschrift.

[10] Raghu Vamsi Krishna Chavali, James Moore, Xufeng Wang, Muhammad Alam, M.s Lundstrom, and Jeffery Gray. The frozen potential approach to separate the photocurrent and diode injection current in solar cells. *Photovoltaics, IEEE Journal of*, 5:865–873, 05 2015. doi: 10.1109/JPHOTOV.2015.2405757.

[11] Rongrong Cheacharoen, Nicholas Rolston, Duncan Harwood, Kevin Bush, Reinhold Dauskardt, and Michael Mcgehee. Design and understanding of encapsulated perovskite solar cells to withstand temperature cycling. *Energy Environ. Sci.*, 11, 10 2017. doi: 10.1039/C7EE02564E.

[12] Yu Chen, Jianchao Yang, Wang Shubo, Yihui Wu, Ningyi Yuan, and Wen-Hua Zhang. Interfacial contact passivation for efficient and stable cesium-formamidinium double-cation lead halide perovskite solar cells. *iScience*, 23:100762, 12 2019. doi: 10.1016/j.isci.2019.100762.

[13] H. et al. Cho. High-efficiency polycrystalline perovskite light-emitting diodes based on mixed cations. 2018. URL https://pubs.acs.org/doi/full/10.1021/acsnano.8b00409.

[14] Jeffrey Christians, Joseph Manser, and Prashant Kamat. Best practices in perovskite solar cell efficiency measurements. avoiding the error of making bad cells look good. *Journal of Physical Chemistry Letters*, 6:852–857, 03 2015. doi: 10.1021/acs.jpclett.5b00289.

[15] Alexander Cimaroli, Yue Yu, Changlei Wang, Weiqiang Liao, Lei Guan, Corey Grice, Dewei Zhao, and Yanfa Yan. Tracking the maximum power point of hysteretic perovskite solar cells using a predictive algorithm. *J. Mater. Chem. C*, 5, 09 2017. doi: 10.1039/C7TC03482B.

[16] B. et al Conings. Intrinsic thermal instability of methylammonium lead trihalide perovskite. 2015. URL https://doi.org/10.1002/aenm.201500477.

[17] A. Mette D. Pysch and S. Glunz. A review and comparison of different methods to determine the series resistance of solar cells. *Solar Energy Materials and Solar Cells*, page 1698 – 1706, 2007. URL https://www.sciencedirect.com/science/article/pii/S0927024807002255.

[18] S. et al De Wolf. Organometallic halide perovskites: Sharp optical absorption edge and its relation to photovoltaic performance. 2014. URL https://pubs.acs.org/doi/10.1021/jz500279b.

[19] Cacovich S. Matteocci F. et al. Divitini, G. In situ observation of heat-induced degradation of perovskite solar cells. 2016. URL https://doi.org/10.1038/nenergy.2015.12.

[20] Zou Y. Song J. Song X. Zeng H Dong, Y. Recent progress of metal halide perovskite photodetectors. 2017. URL https://pubs.rsc.org/en/content/articlelanding/2017/tc/c7tc03612d#!divAbstract.

[21] Ricky Dunbar, Walied Moustafa, Alexander Pascoe, Timothy Jones, Kenrick Anderson, Cheng Bing, Christopher Fell, and Gregory Wilson. Device pre□conditioning and steady□state temperature dependence of ch3nh3pbi3 perovskite solar cells. *Progress in Photovoltaics: Research and Applications*, 25, 11 2016. doi: 10.1002/pip.2839.

[22] Allebé C. Remo T. et al Essig, S. Raising the one-sun conversion efficiency of iii–v/si solar cells to 32.8% for two junctions and 35.9% for three junctions. 2017. URL https://www.nature.com/articles/nenergy2017144.

[23] Solar Power Europe. Global market outlook. 2020. URL https://www.solarpowereurope.org/wp-content/uploads/2021/07/SolarPower-Europe_Global-Market-Outlook-for-Solar-2021-2025_V1.pdf.

[24] J.G.Fossum F.A.Lindholm and E.L.Burgess. Application of the superposition principle to solar-cell analysis. *IEEE TRANSACTIONS ON ELECTRON DEVICE*, 26(3):165–171, 1979. doi: https://doi.org/10.1109/T-ED.1979.19400.

[25] John C.C. Fan. Theoretical temperature dependence of solar cell parameters. *Solar Cells*, 17:309–315, 1986. ISSN 0379-6787. doi: https://doi.org/10.1016/0379-6787(86)90020-7.

[26] Ben Foley, Daniel Marlowe, Keye Sun, Wissam Saidi, Louis Scudiero, Mool Gupta, and Joshua Choi. Temperature dependent energy levels of methylammonium lead iodide perovskite. *Applied Physics Letters*, page 243904, 06 2015. doi: 10.1063/1.4922804.

[27] Jenkins C.R. Sites J.R Gloeckler, M. Explanation of light/dark superposition failure in cigs solar cells. *MRS Online Proceedings Library, 763,B5.20.*

[28] Ho-Baillie A. Snaith H Green, M. The emergence of perovskite solar cells. 2014. URL https://doi.org/10.1038/nphoton.2014.134.

[29] M. A. Green and A. W. Blakers. Characterization of high-efficiency silicon solar cells. *Journal of Applied Physics*, 58:4402–4408, 11 1985. doi: 10.1063/1.336286.

[30] Martin Green, Yoshihiro Hishikawa, Ewan Dunlop, Dean Levi, Jochen Hohl-Ebinger, and Anita Ho-Baillie. Solar cell efficiency tables (version 52). *Progress in Photovoltaics: Research and Applications*, 26:427–436, 07 2018. doi: 10.1002/pip.3040.

[31] Martin A. Green. Accuracy of analytical expressions for solar cell fill factors. 7:337–340, 1982. ISSN 0379-6787. URL https://doi.org/10.1016/0379-6787(82)90057-6.

[32] Oki Gunawan, Tayfun Gokmen, and David Mitzi. Suns-voc characteristics of high performance kesterite solar cells. *Journal of Applied Physics*, 116, 06 2014. doi: 10.1063/1.4893315.

[33] H.D.Kim and H.Ohkita. Potential improvement in fill factor of lead-halide perovskite solar cells. *Solar RRL*, 1, 2017. doi: https://doi.org/10.1002/solr.201700027.

[34] M Jaysankar. *Multijunction solar cells based on hybrid perovskites*. PhD thesis, Jan 2019. URL https://limo.libis.be/primo-explore/fulldisplay?docid=LIRIAS2342810&context=L&vid=Lirias&search_scope=Lirias&tab=default_tab&lang=en_US&fromSitemap=1.

[35] Noh-J. Kim Y. et al Jeon, N. Solvent engineering for high-performance inorganic-organic hybrid perovskite solar cells. 2014. URL https://doi.org/10.1038/nmat4014.

[36] Jaeki Jeong, Minjin Kim, Jongdeuk Seo, Haizhou Lu, Paramvir Ahlawat, Aditya Mishra, Yingguo Yang, Michael Hope, Felix Eickemeyer, Maengsuk Kim, Yung Yoon, In Choi, Barbara Darwich, Seung Choi, Yimhyun Jo, Jun Lee, Bright Walker, Shaik Zakeeruddin, Lyndon Emsley, and Jin Young Kim. Pseudo-halide anion engineering for α-fapbi3 perovskite solar cells. *Nature*, 592:1–5, 04 2021. doi: 10.1038/s41586-021-03406-5.

[37] Mingyu Jeong, In Choi, Eun Go, Yongjoon Cho, Minjin Kim, Byongkyu Lee, Seonghun Jeong, Yimhyun Jo, Hye Choi, Jiyun Lee, Jin-Hyuk Bae, Sang Kyu Kwak, Dong Kim, and Changduk Yang. Stable perovskite solar cells with efficiency exceeding 24.8% and 0.3-v voltage loss. *Science (New York, N.Y.)*, 369:1615–1620, 09 2020. doi: 10.1126/science.abb7167.

[38] Marko Jošt, Benjamin Lipovšek, Boštjan Glažar, Amran Al-Ashouri, Kristijan Brecl, Gašper Matič, Artiom Magomedov, Vytautas Getautis, Marko Topic, and Steve Albrecht. Perovskite solar cells go outdoors: Field testing and temperature effects on energy yield. *Advanced Energy Materials*, 10, 05 2020. doi: 10.1002/aenm.202000454.

[39] J.-L. Song K. Chu, Y.-H. Zhou and C. Zhang. An abx 3 organic-inorganic perovskite-type material with the formula (c5n2h9)cdcl 3 : Application for detection of volatile organic solvent molecules. 2017. URL https://www.researchgate.net/publication/316476986_An_ABX_3_Organic-Inorganic_Perovskite-Type_Material_with_the_Formula_C_5_N_2_H_9_CdCl_3_Application_for_Detection_of_Volatile_Organic_Solvent_Molecules.

[40] D. D. Ceuster K. Wilson and R. A. Sinton. Measuring the effect of cell mismatch on module output. *IEEE 4th World Conference on Photovoltaic Energy Conference*, pages 916–919, 2006. doi: 10.1109/WCPEC.2006.279605.

[41] Brendan Kayes, Hui Nie, Rose Twist, S. Spruytte, Frank Reinhardt, Isik Kizilyalli, and Gregg Higashi. 27.6% conversion efficiency, a new record for single-junction solar cells under 1 sun illumination. *Conference Record of the IEEE Photovoltaic Specialists Conference*, pages 000004–000008, 06 2011. doi: 10.1109/PVSC.2011.6185831.

[42] Robert Kenny, Anatoli Chatzipanagi, and Tony Sample. Preconditioning of thin-film pv module technologies for calibration. *Progress in Photovoltaics: Research and Applications*, 2, 02 2014. doi: 10.1002/pip.2234.

[43] T.Hoshino K.H.Hussein, I.Muta and M.Osakada. Maximum photovoltaic power tracking: an algorithm for rapidly changing atmospheric conditions. 1995. URL https://doi.org/10.1049/IP-GTD:19951577.

[44] A. Killam and S. Bowden. Characterization of modules and arrays with suns voc. pages 2719–2722, 2017. doi: 10.1109/PVSC.2017.8366428.

[45] National Renewable Energy Laboratory. Best research-cell efficiencies chart. 2020. URL https://www.nrel.gov/pv/cell-efficiency.html.

[46] Mehdi Leilaeioun and Zachary Holman. Accuracy of expressions for the fill factor of a solar cell in terms of open-circuit voltage and ideality factor. *Journal of Applied Physics*, 120:123111, 09 2016. doi: 10.1063/1.4962511.

[47] Wei Leong, Zi-En Ooi, Dharani Sabba, Chenyi Yi, Shaik Zakeeruddin, Michael Graetzel, Jeffrey Gordon, Eugene Katz, and Nripan Mathews. Identifying fundamental limitations in halide perovskite solar cells. *Advanced materials (Deerfield Beach, Fla.)*, 28, 01 2016. doi: 10.1002/adma.201505480.

[48] Fossum J. G.-Burgess E. L. Lindholm, F. A. Basic corrections to predictions of solar cell performance required by nonlinearities. pages 33–39, 1976.

[49] R Lindsey. Climate change: Atmospheric carbon dioxide. August 2020. URL https://www.climate.gov/news-features/understanding-climate/climate-change-atmospheric-carbon-dioxide.

[50] LMPV. Detailed balance (db) charts. 2021. URL https://www.lmpv.nl/db/.

[51] Giovanni Mannino, Alessandra Alberti, Ioannis Deretzis, Emanuele Smecca, Salvatore Sanzaro, Youhei Numata, Tsutomu Miyasaka, and Antonino Magna. First evidence of ch 3 nh 3 pbi 3 optical constant improvement in n 2 environment in the range 40-80 °c. *The Journal of Physical Chemistry C*, 121, 03 2017. doi: 10.1021/acs.jpcc.7b00764.

[52] P. Zhai H.O. Pörtner D. Roberts J. Skea P.R. Shukla A. Pirani W. Moufouma-Okia C. Péan R. Pidcock S. Connors J.B.R. Matthews Y. Chen X. Zhou M.I. Gomis E. Lonnoy T. Maycock M. Tignor Masson-Delmotte, V. and T. Waterfield. Ipcc, 2018: Global warming of 1.5°c. 2018. URL https://www.ipcc.ch/site/assets/uploads/sites/2/2019/06/SR15_Full_Report_High_Res.pdf.

[53] Owen Miller, Eli Yablonovitch, and Sarah Kurtz. Strong internal and external luminescence as solar cells approach the shockley–queisser limit. *Photovoltaics, IEEE Journal of*, 2:303–311, 07 2012. doi: 10.1109/JPHOTOV.2012.2198434.

[54] W. Yang Y. Kim S. Ryu J. Seo N. Jeon, J. Noh and S. Seok. Compositional engineering of perovskite materials for high-performance solar cells. 2015. URL https://pubmed.ncbi.nlm.nih.gov/25561177/.

[55] M.A. Green Olivier Dupré, RODOLPHE VAILLON. *Thermal Behavior of Photovoltaic Devices*. 2017. URL https://link.springer.com/content/pdf/10.1007/978-3-319-49457-9.pdf.

[56] C R Osterwald, T Glatfelter, and J Burdick. Comparison of the temperature coefficients of the basic i-v parameters for various types of solar cells. 1 1987. URL https://www.osti.gov/biblio/978922.

[57] Norman Pellet, Fabrizio Giordano, M Ibrahim Dar, Giuliano Gregori, Shaik Zakeeruddin, Joachim Maier, and Michael Graetzel. Hill climbing hysteresis of perovskite-based solar cells: a maximum power point tracking investigation: Maximum power point tracking of perovskite-based solar cells. *Progress in Photovoltaics: Research and Applications*, 25, 06 2017. doi: 10.1002/pip.2894.

[58] S. P. Philipps, R. Hoheisel, T. Gandy, D. Stetter, M. Hermle, F. Dimroth, and A. W. Bett. An experimental and theoretical study on the temperature dependence of gaas solar cells. pages 001610–001614, 2011. doi: 10.1109/PVSC.2011.6186264.

[59] N.M. Ravindra Priyanka Singh. Temperature dependence of solar cell performance—an analysis. *Applied Physics Letters*, pages 36–45, 2012. doi: 10.1016/j.solmat.2012.02.019. URL https://www.sciencedirect.com/science/article/pii/S0927024812000931.

[60] Oxford PV. Oxford pv hits new world record for solar cell. 2021. URL https://www.oxfordpv.com/news/oxford-pv-hits-new-world-record-solar-cell.

[61] Damian Pysch, Ansgar Mette, and Stefan Glunz. A review and comparison of different methods to determine the series resistance of solar cells. *Solar Energy Materials and Solar Cells*, 91:1698–1706, 11 2007. doi: 10.1016/j.solmat.2007.05.026.

[62] M. S. Lundstrom R. J. Schwartz and R. D. Nasby. The degradation of high-intensity bsf solar-cell fill factors due to a loss of base conductivity modulation. *IEEE Trans. Electron Devices*, 28(3):264–269, 1981. doi: https://doi.org/10.1109/T-ED.1981.20325.

[63] Thomas Roth, Jochen Hohl-Ebinger, Daniela Grote, Evelyn Schmich, Wilhelm Warta, Stefan Glunz, and Ronald Sinton. Illumination-induced errors associated with suns-voc measurements of silicon solar cells. *The Review of scientific instruments*, 80:033106, 04 2009. doi: 10.1063/1.3095441.

[64] V. Yelundur S. Bowden and A. Rohatgi. Implied-voc and suns-voc measurements in multicrystalline solar cells. *Proceedings of the 29th IEEE Photovoltaic Specialists Conference*, 2002.

[65] H. Mäckel S. W. Glunz, J. Nekarda and A. Cuevas. Analyzing back contacts of silicon solar cells by suns-voc-measurements at high illumination densities. *Proceedings of the 22nd European Photovoltaic Solar Energy Conference Milan, Italy*, pages 849–853, 2007. URL http://publica.fraunhofer.de/eprints/urn_nbn_de_0011-n-734673.pdf.

[66] P.R.Nair S.Agarwal. Device engineering of perovskite solar cells to achieve near ideal efficiency. *Applied Physics Letters*.

[67] Hidenori SAITO, Daisuke AOKI, Tomoyuki TOBE, and Shinichi MAGAINO. Development of a new maximum power point tracking method for power conversion efficiency measurement of metastable perovskite solar cells. *Electrochemistry*, 88, 04 2020. doi: 10.5796/electrochemistry.20-00022.

[68] Michael Saliba, Taisuke Matsui, Ji-Youn Seo, Konrad Domanski, Juan-Pablo Correa-Baena, Mohammad Nazeeruddin, Shaik Zakeeruddin, Wolfgang Tress, Antonio Abate, Anders Hagfeldt, and Michael Gratzel. Cesium-containing triple cation perovskite solar cells: Improved stability, reproducibility and high efficiency. *Energy Environmental Science*, 03 2016. doi: 10.1039/C5EE03874J.

[69] José Domingo Santos Rodríguez and Jose Balenzategui. I-v characterization of solar cells with variable intensity monochromatic light. 09 2008.

[70] Sebastian Schiefer, Birger Zimmermann, and Uli Würfel. Determination of the intrinsic and the injection dependent charge carrier density in organic solar cells using the suns-voc method. *Journal of Applied Physics*, 115:–, 01 2014. doi: 10.1063/1.4862960.

[71] J.J. Schoeman and J.D. van Wyk. A simplified maximal power controller for terrestrial photovoltaic panel arrays. pages 361–367, 1982. doi: 10.1109/PESC.1982.7072429.

[72] Wei Sha, Xingang Ren, Luzhou Chen, and Wallace Choy. The efficiency limit of ch3nh3pbi3 perovskite solar cells. *Applied Physics Letters*, 106:221104, 06 2015. doi: 10.1063/1.4922150.

[73] Queisser H.J. Shockley, W. Detailed balance limit of efficiency of p-n junction solar cells. 1961. URL https://aip.scitation.org/doi/10.1063/1.1736034.

[74] Priyanka Singh and Nuggehalli Ravindra. Temperature dependence of solar cell performance - an analysis. *Solar Energy Materials and Solar Cells*, 101:36–45, 06 2012. doi: 10.1016/j.solmat.2012.02.019.

[75] R.A. Sinton and A. Cuevas. A quasi-steady-state open-circuit voltage method for solar cell characterization. *16th European Photovoltaic Solar Energy Conference. Glasgow, Scotland*, page 1152–1155, 2000. URL https://www.sintoninstruments.com/wp-content/uploads/sinton-epvsc16-pcd.pdf.

[76] Henry Snaith, Antonio Abate, James Ball, Giles Eperon, Tomas Leijtens, Nakita Noel, Samuel Stranks, Jacob Wang, Konrad Wojciechowski, and Wei Zhang. Anomalous hysteresis in perovskite solar cells. *Journal of Physical Chemistry Letters*, 5:1511–1515, 03 2014. doi: 10.1021/jz500113x.

[77] S.W.Glunz U.Würfel S.Schiefer, B.Zimmermann. Applicability of the suns-voc method on organic solar cells. *IEEE Journal of Photovoltaics*, 4, 01 2014. doi: 10.1109/JPHOTOV.2013.2288527.

[78] Martin Stolterfoht, Christian Wolff, Yohai Amir, Andreas Paulke, Lorena Perdigón Toro, Pietro Caprioglio, and Dieter Neher. Approaching the fill factor shockley queisser limit in stable, dopant-free triple cation perovskite solar cells. *Energy Environ. Sci.*, 10, 05 2017. doi: 10.1039/C7EE00899F.

[79] M. G. Halide Perovskites Stoumpos, C. C. Kanatzidis. Halide perovskites: Poor man's high□performance semiconductors. 2016. URL https://doi.org/10.1002/adma.201600265.

[80] Snaith H Stranks, S. Metal-halide perovskites for photovoltaic and light-emitting devices. 2015. URL https://doi.org/10.1038/nnano.2015.90.

[81] Peidong Su, Yu Liu, Junke Zhang, Cong Chen, Bo Yang, Chunhui Zhang, and Xu Zhao. Pb-based perovskite solar cells and the underlying pollution behind clean energy: Dynamic leaching of toxic substances from discarded perovskite solar cells. *The Journal of Physical Chemistry Letters*, 11:2812–2817, 04 2020. doi: 10.1021/acs.jpclett.0c00503.

[82] Anshu Sharma Arvind S.P. Nehra M.S. Dhaka Subhash Chander, A. Purohit. A study on photovoltaic parameters of mono-crystalline silicon solar cell with cell temperature. *Energy Reports*, 1:104–109, 2015. ISSN 2352-4847. doi: https://doi.org/10.1016/j.egyr.2015.03.004.

[83] N. G. TARR and D. L. PULFREY. An investigation of dark current and photocurrent superposition in photovoltaic devices. *Solid-State Electronics*.

[84] N. G. Tarr and D. L. Pulfrey. The superposition principle for homojunction solar cells. *IEEE Trans. Electron Devices*, 27(4):771–776, 1980. doi: https://doi.org/10.1109/T-ED.1980.19935.

[85] Zhou H. Li L Tian, W. Hybrid organic–inorganic perovskite photodetectors. 2017. URL https://doi.org/10.1002/smll.201702107.

[86] Liang Tian Shen, Mauro Pravettoni, Jai Prakash Singh, and Yong Sheng Khoo. Meeting the requirements of iec ts 60904-1-2 for single light source bifacial photovoltaic characterisation: evaluation of different back panel materials. *Engineering Research Express*, 2, 03 2020. doi: 10.1088/2631-8695/ab7ee5.

[87] Eva Unger, Eric Hoke, Colin Bailie, William Nguyen, Andrea Bowring, Thomas Heumueller, Mark Christoforo, and Michael Mcgehee. Hysteresis and transient behavior in current-voltage measurements of hybrid-perovskite absorber solar cells. *Energy Environ. Sci.*, 7, 08 2014. doi: 10.1039/C4EE02465F.

[88] Changlei Wang, Chuanxiao Xiao, Yue Yu, Dewei Zhao, Rasha Awni, Corey Grice, Kiran Ghimire, Iordania Constantinou, Weiqiang Liao, Alexander Cimaroli, Pei Liu, Jing Chen, Nikolas Podraza, Chun-Sheng Jiang, Mowafak Al-Jassim, Xingzhong Zhao, and Yanfa Yan. Understanding and eliminating hysteresis for highly efficient planar perovskite solar cells. *Advanced Energy Materials*, 7, 05 2017. doi: 10.1002/aenm.201700414.

[89] Jérémie Werner, Loris Barraud, Arnaud Walter, Matthias Bräuninger, Florent Sahli, Davide Sacchetto, Nicolas Tétreault, Bertrand Paviet-Salomon, Soo-Jin Moon, Christophe Allebé, Matthieu Despeisse, Sylvain Nicolay, Stefaan De Wolf, Bjoern Niesen, and Christophe Ballif. Efficient near-infrared-transparent perovskite solar cells enabling direct comparison of 4-terminal and monolithic perovskite/silicon tandem cells. *ACS Energy Letters*, 1, 07 2016. doi: 10.1021/acsenergylett.6b00254.

[90] Niesen B. Ballif C. Werner, J. Perovskite/silicon tandem solar cells: Marriage of convenience or true love story? – an overview. 2018. URL https://onlinelibrary.wiley.com/doi/abs/10.1002/admi.201700731.

[91] M. Wolf and H. Rauschenbach. Series resistance effects on solar cell measurements. *Advanced Energy Conversion*, 3:455–479, 1963.

[92] Eli Yablonovitch, Owen Miller, and Sarah Kurtz. The opto-electronic physics that broke the efficiency limit in solar cells. *Conference Record of the IEEE Photovoltaic Specialists Conference*, pages 001556–001559, 06 2012. doi: 10.1109/PVSC.2012.6317891.

[93] Yourim Yoon and Zong Woo Geem. Parameter optimization of single-diode model of photovoltaic cell using memetic algorithm. *International Journal of Photoenergy*, 2015:1–7, 11 2015. doi: 10.1155/2015/963562.

[94] Kunta Yoshikawa, Hayato Kawasaki, Wataru Yoshida, Toru Irie, Katsunori Konishi, Kunihiro Nakano, Toshihiko Uto, Daisuke Adachi, Masanori Kanematsu, Hisashi Uzu, and Kenji Yamamoto. Silicon heterojunction solar cell with interdigitated back contacts for a photoconversion efficiency over 26%. *Nature Energy*, 2:17032, 03 2017. doi: 10.1038/nenergy.2017.32.

[95] Hua Zhang, Xianfeng Qiao, Yan Shen, Thomas Moehl, Shaik Zakeeruddin, Michael Graetzel, and Mingkui Wang. Photovoltaic behaviour of lead methylammonium triiodide perovskite solar cells down to 80 k. *J. Mater. Chem. A*, 3, 04 2015. doi: 10.1039/C5TA02206A.

[96] Xu.J Zhu.M, Mao.K. Perovskite tandem solar cells with improved efficiency and stability. July 2020. URL https://www.sciencedirect.com/science/article/pii/S2095495620306574#f0010.